Seismic stratigraphy, structure and tectonic evolution of the Levantine Basin, offshore Israel

MICHAEL A. GARDOSH & YEHEZKEL DRUCKMAN

The Geophysical Institute of Israel, POB 182, Lod 71100, Israel (e-mail: miki@gii.co.il)

Abstract: Multi-channel seismic reflection data and borehole information were used to study the structure and stratigraphy of the Levantine basin, offshore Israel. A new, 2D seismic survey that covers the southeastern Mediterranean Sea from the Israeli coast to the Eratosthenes Seamount shows the entire Phanerozoic sedimentary fill down to a depth of 14–16 km. The basin-fill is subdivided into six seismo-stratigraphic units interpreted as low-order, major depositional cycles (supersequences A–F). Correlation and mapping of these units allowed an investigation of the geological history of the basin and the analysis of two important tectonic phases: Neotethyan rifting, and Syrian Arc inversion and contraction. The Neotethyan rifting phase is recorded by the strata of supersequences A and B. Faulting took place during the Anisian (Mid-Triassic), continued through the Liassic and ceased during the Mid-Jurassic. The basin opened in a NW–SE direction, between the Eratosthenes Seamount and the Levant margin of the Arabian Massif, at an angle of about 30° to the present-day shoreline. No indications for sea-floor spreading were found in the present study. Late Triassic to Liassic volcanic rocks of assumed intraplate origin accumulated in the northeastern part of the basin. It is hypothesized that the basin originated as an intracontinental rift associated with the nucleation of an oceanic spreading centre, but reached only an early magmatic phase. An inversion and contraction phase, associated with closing of the Neotethyan ocean system, is recorded by supersequences C and D. The contractional structures of the Syrian Arc extend in a wide and elevated fold belt along the eastern edge of the deep-marine basin. These structures were formed by the inversion of pre-existing normal faults. The folding occurred in several pulses starting in the Senonian and ending in the Miocene. The western limit of the main fold belt, located 50–70 km west of the coastline, is defined by a transition in crustal properties. Supersequences E and F record the Late Cenozoic history of the basin. A Messinian, evaporitic basin was limited to the east by the elevated and uplifted Syrian Arc fold belt composed of older, Oligocene to Mid-Miocene strata. During highstand episodes, the Messinian evaporites were deposited on the entire slope and within canyons incised into the shelf. High sedimentation rates of Nilotic and locally derived sediments during the Plio-Pleistocene resulted in the development of extensive submarine deltas and basinward progradation of the Levant shelf break.

The Levantine basin (Fig. 1a) occupies a considerable part of the eastern Mediterranean Sea. It is bounded to the east and south by the continental slopes of the African and Arabian plates along the Mediterranean coast of Sinai, Israel, Lebanon and Syria, and on the north by the Cyprian Arc plate boundary at the southern edge of Eurasia. It is a deep marine basin reaching water depth of up to 2200 m below mean sea level (MSL).

The basin is a remnant of the Neotethys Ocean that opened following the break-up of Pangaea in Early Mesozoic times (Dewey *et al.* 1973; Robertson & Dixon 1984). During the Mid–Late Cretaceous the basin started to close. The northern margins were intensely deformed and subsequently subducted or accreted at the present-day areas of Cyprus and southern Turkey (Fig. 1) (Ben Abraham 1989; Garfunkel 1998; Robertson 1998). The southeastern margins, however, remained stable at their original position near the Israel–Sinai coastline. The sedimentary sections on the slope and deep-marine basin of the southeastern Levant continental margin preserve important evidence of events associated with the opening and closing of the Neotethys.

A vast volume of geological and geophysical data that were collected in the past 40 years have been used to study the structure and stratigraphy of the Levantine basin and to develop a conceptual model to explain its origin and tectonic evolution. The existence of a deep sedimentary basin in the southeastern Mediterranean Sea area was initially revealed during the late 1960s to 1980s (Ginzburg *et al.* 1975; Neev *et al.* 1976; Bein & Gvirtzman 1977; Druckman 1984; Garfunkel & Derin 1984; Cohen *et al.* 1988, 1990).

From: ROBERTSON, A. H. F. & MOUNTRAKIS, D. (eds) 2006. *Tectonic Development of the Eastern Mediterranean Region*. Geological Society, London, Special Publications, **260**, 201–227.
0305-8719/06/$15.00

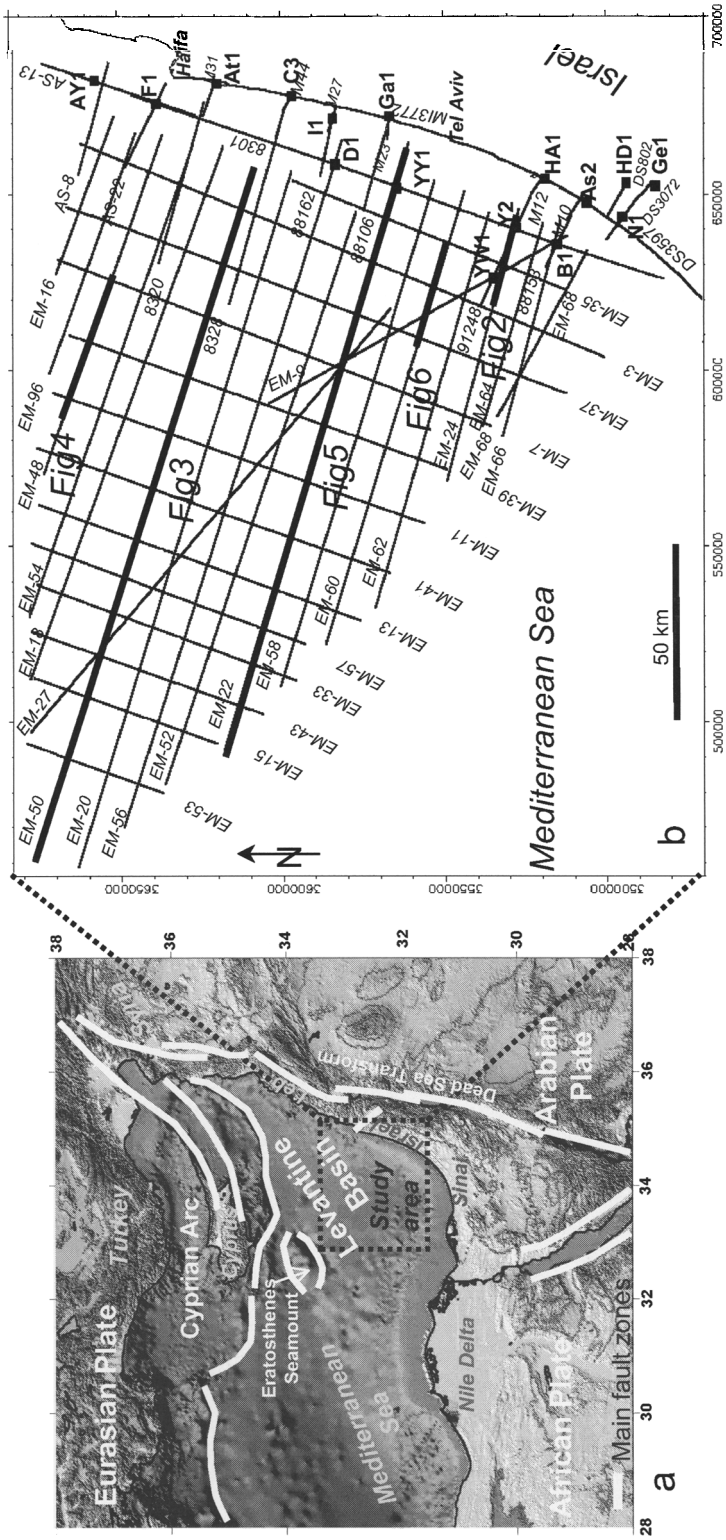

Fig. 1. Location map of the study area. (**a**) Satellite image showing the physiography and main tectonic elements of the eastern Mediterranean region. The Levantine basin is a deep-marine basin located west and north of the African and Arabian continental slopes and south of the Eratosthenes Seamount and Cyprian Arc plate boundary. (**b**) Location of the studied seismic reflection profiles and deep boreholes in the southeastern Mediterranean Sea and coastal plain of Israel. Well abbreviations: AY1, Asher Yam-1; As2, Ashkelon-2; At1, Atlit-1; B1, Bravo-1; C3, Caesarea-3; D1, Delta-1; F1, Foxtrot1; Ga-2, Gaash-2; Ge1, Gevim-1; HD1, Heletz Deep-1; HA1, Hof Ashdod-1; I1, Item-1; N1, Nisanit-1; YW1, Yam West-1; YY1, Yam Yafo-1; Y2, Yam-2.

Studies of onshore and offshore deep boreholes have shown marked lateral changes in the Jurassic and Cretaceous rock record, and a transition from shallow-marine shelf and slope facies in the south and east to deep marine facies in the west. Multi-channel seismic reflection surveys shot on the continental shelf have confirmed the presence of a thick Mesozoic to Neogene rock succession that extends throughout the southeastern Mediterranean area. The deep sedimentary basin and its bordering land were interpreted as a relic of the Neotethys Ocean and adjacent passive continental margin that developed on the northern edge of the Arabian plate in Early Mesozoic times (Fig. 1).

The relation between the sedimentary rock record and the deep crustal structure was studied on a regional scale in a later phase of research. Long-range seismic refraction profiles and gravity and magnetic data were collected over the inland part of Israel and across the southeastern Mediterranean Sea, and revealed considerable variations in the density and velocity of the crust (Ginzburg *et al.* 1979; Ginzburg & Folkman 1980; Makris *et al.* 1983; Ginzburg & Ben-Avraham 1987; Makris & Wang 1994; Ben-Avraham *et al.* 2002). The geophysical dataset showed a 35 km thick, continental-type crust beneath southern Israel that thins to *c.* 10 km in the central part of the marine basin. The thickness of the sedimentary cover was found to change accordingly from 6 km near the Mediterranean coast to about 15 km in the offshore area. These findings further supported the initial interpretation of the basin as a major tectonic element in the area.

The analysis of gravity and magnetic data, seismic refraction and single-channel seismic reflection data from the northeastern Mediterranean Sea has all revealed more information on the northern edge of the Levantine basin (Fig. 1) (Ben-Avraham *et al.* 1976; Woodside 1977; Makris *et al.* 1983; Makris & Wang 1994; Ben-Avraham *et al.* 1995). The elevated structures of Cyprus and the submarine Eratosthenes Seamount were found to be underlain by a 25–35 km thick crust of assumed continental origin. An area of prominent deformation and wrench faulting found south and east of Cyprus was interpreted as an active boundary between the African–Arabian plate on the south and the Eurasian plate on the north. The uplift and deformation along the Cyprian Arc plate boundary was explained by the closure of the Neotethyan Ocean through plate collision, subduction and accretion processes in the northern part of the Mesozoic Levantine basin. The Eratosthenes Seamount was interpreted as a small continental body detached from the African plate during the Neotethyan rifting and later moved northward to its present location just south of the present plate boundary.

Although many details of the Levantine basin are now well recognized, there is disagreement among researchers regarding several important aspects of its origin and tectonic evolution. An 'oceanic' model assumes that the thin crust found in the central part of the basin is a relic of a Neotethyan oceanic lithosphere. According to this model the Levantine basin evolved since the break-up of Pangaea in Late Permian time as the southern arm of a large Neotethys ocean. Rifting and sea-floor spreading episodes in the Triassic to Early Jurassic were presumably followed by the emplacement of new oceanic crust in the central and northern part of the basin (Bein & Gvirtzman 1977; Makris *et al.* 1983; Ben-Avraham *et al.* 2002).

An alternative 'continental' model suggests that the central part of the basin is composed of thinned continental crust. The Levantine basin is assumed to be underlain by a number of aborted or failed rifts that opened on the Mesozoic shallow shelf, south of the large Neotethyan Ocean (Hirsch *et al.* 1995).

Another area of disagreement is associated with the geometry and nature of opening of the Levantine basin. Based on plate motion reconstruction several workers have suggested an east–west-oriented spreading centre within the basin that separated the Tauride microplate from Africa, and was associated with north–south, strike-slip motion on a transform fault along the eastern coast of the Mediterranean (Dewey *et al.* 1973; Şengör *et al.* 1984; Dercourt *et al.* 1986; Stampfli *et al.* 2001). A NNE-trending discontinuity zone identified in geophysical data along the base of the Israeli continental shelf, termed the Pelusium Line, was interpreted as a major transcontinental shear associated with the postulated north–south strike-slip motion (Neev *et al.* 1976; Neev 1977).

An alternative view proposes a north–south-oriented spreading centre within the basin and a NW–SE extension and opening between the Mediterranean coastline and the Eratosthenes and Cyprus areas. This model postulates an east–west, strike-slip motion along the northern coast of Sinai (Garfunkel & Derin, 1984; Garfunkel, 1998).

Hydrocarbon exploration activity has taken place in the Levantine basin, offshore Israel since the 1970s. In the last 10 years, following a renewed interest in its hydrocarbon potential and significant gas discoveries, a large amount of geophysical data were collected across the marine

basin and several deep wells were drilled in the eastern margin. The new data provide a detailed and more accurate image of the subsurface that was not previously available.

This paper presents an analysis of part of the new geophysical dataset. It focuses primarily on a regional 2D seismic reflection survey performed across the southeastern Mediterranean Sea during 2001. A seismic stratigraphic analysis was used to define and map the main rock units that make up the basin-fill. Several regional fault and fold systems were identified in the basin and on its margin. The results are used to evaluate and update the models previously suggested to explain the tectonic evolution and geological history of the Levantine basin.

Dataset

The seismic dataset used in this research includes 52 multi-channel, 2D seismic reflection lines totalling 4000 km. The core of the study is a grid of 32 regional marine lines acquired during 2001 in the framework of hydrocarbon exploration activity offshore Israel (EM series in Fig. 1b). These data, obtained by Spectrum Energy and Information Technology Ltd, extend from the Israeli shallow shelf to the submarine Eratosthenes Seamount, some 200 km to the NW. It covers most of the Levantine basin in a relatively dense seismic grid of about 10 km × 20 km (Fig. 1b). The EM lines were acquired by the R.V. *Geo Baltic* vessel using a 7200 m long streamer with 576 recording channels (group interval 12.5 m), and an energy source of a four air gun array, each gun with a volume of 3410 cubic inches and a pressure of 3000 p.s.i. The optimal shooting parameters and data processing sequence resulted in a highly interpretable dataset in which seismic reflections are well resolved down to about 10s two-way travel time (TWT; Figs 2–6). The resolution and depth of penetration of the new EM series is superior to most other 2D reflection lines previously acquired for offshore Israel.

Twenty additional 2D multi-channel reflection lines of older vintages were reprocessed and integrated into the seismic dataset (DS, AS, M, 83, 88 and 91 series in Fig. 1b). These lines, which cover nearshore and onshore areas, allowed the correlation of the seismic data to 16 deep boreholes located on the eastern margin of the basin (Fig. 1, Table 1).

An interpretation of the entire seismic dataset was performed on a workstation using time-migrated profiles. Synthetic seismograms and time-converted wireline logs were constructed for the correlation of seismic horizons to stratigraphic units in the wells. Biostratigraphic and lithostratigraphic information, taken from published well reports, was used for age control and the geological interpretation of seismic events.

Seismic stratigraphy

Seismic interpretation and mapping

A thick reflection series (up to 10 s TWT) comprises the entire sedimentary rock record that accumulated on the northern edge of the Arabian–African plate during the Phanerozoic (Figs 2–6). Six seismic packages were identified in the Phanerozoic sedimentary interval, between the crystalline basement and the water bottom surface (Fig. 2). The packages are distinct seismic units that are bounded by regional markers recognized through truncation and both onlapping and downlapping reflections. Correlation with deep boreholes shows that the seismic packages comprise major lithostratigraphic units (Fig. 2) and their boundaries are regional unconformity surfaces associated with relative sea-level changes.

The seismo-stratigraphic units were interpreted as low-order depositional cycles that developed in response to the main tectonic events that shaped the Levantine basin and margin. The time span of most of these depositional cycles, labelled from bottom to top as units A to F (Fig. 2), ranges from 5 to about 80 Ma. According to sequence stratigraphic terminology they are defined as second-order depositional sequences or supersequences (Haq *et al.* 1988; Emery & Myers 1996). Supersequence E, comprising the Messinian evaporate, is a higher-order depositional cycle with a time span of <2 Ma. However, the Messinian strata represents a conspicuous seismic and lithostratigraphic unit that is well recognized throughout the basin and is therefore described here, for simplicity, within the supersequence scheme.

Mapping of supersequences A–F involved several steps. First, time–structure and time–thickness grids (isochrons) were prepared for each of the interpreted seismic horizons. The isochron grids were converted to isopach maps by multiplication of one-way travel time values by a single interval velocity (Fig. 7a–f). The isopach maps were then summed (in a layer-cake manner) to create the depth maps of the various unit tops (Fig. 8a and b).

Seismic interval velocities used for depth conversion were calculated from check shot surveys of the 16 deep wells in the study area (Table 1,

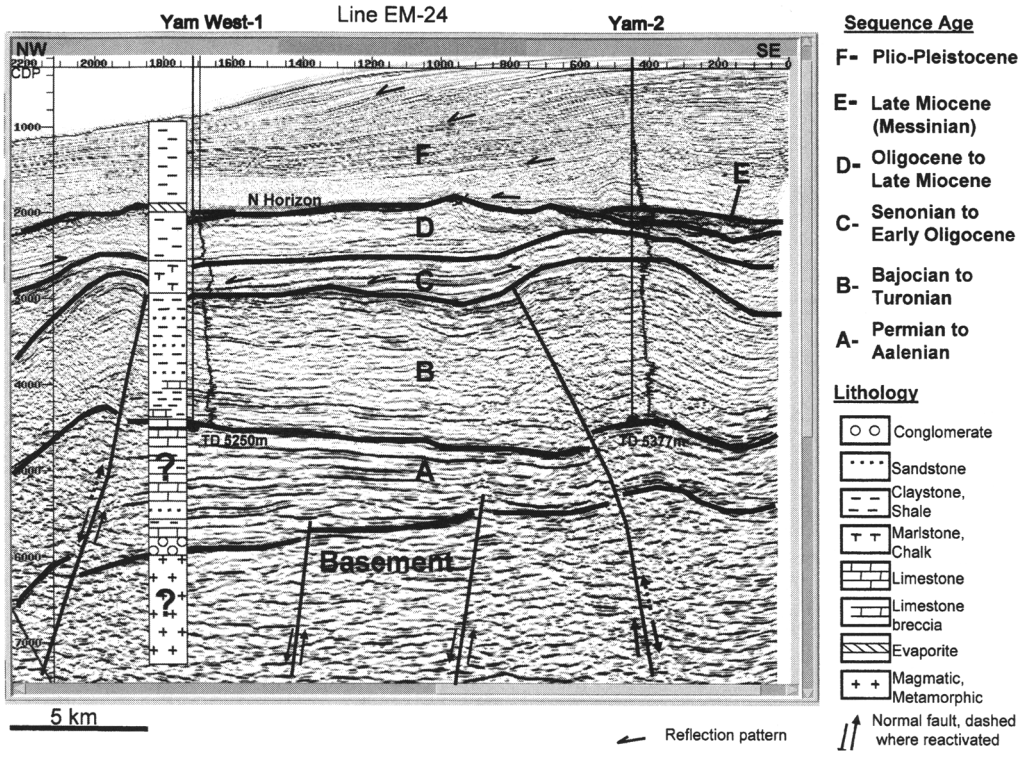

Fig. 2. Interpreted, time-migrated seismic reflection line EM-24 (eastern part), showing the six seismo-stratigraphic units composing the Phanerozoic sedimentary fill of the Levantine basin (supersequences A–F). Each supersequence is dominated by a unique seismic facies: A is a series of parallel, high-amplitude reflections above the chaotic crystalline basement; B is characterized by discontinuous, low-amplitude reflections and reflection-free zones; C is a series of parallel, continuous reflections, in places onlapping the top of B; D is characterized by discontinuous, low-amplitude reflections; E is chaotic to reflection-free (Messinian evaporite); F is composed of a thinly layered, basinward-prograding reflection pattern. The supersequence boundaries are correlated with regional unconformity surfaces that are dated in onshore and offshore wells. An interpreted lithological column of the basin-fill is partly taken from cutting sample description of the Yam West-1 well. The composition of the Precambrian basement and the overlying supersequence A is assumed based on seismic character and the extrapolation from nearby onshore wells. CDP, common depth point. Location of the seismic profile and the wells is shown in Figure 1b.

Fig. 1). The velocity data available for time to depth conversion are limited and come only from the shallow, eastern part of the basin (Fig. 1b). Therefore, the following approximations are required: an interval velocity of 4200 m s^{-1} was used for depth conversion of the Messinian evaporates, as the velocity calculated for this interval from the Yam-2 well (3311 m s^{-1}) is considered unrepresentative (Table 1); units D and C have similar compositions; both are dominated by argillaceous limestone and chalk, therefore, the same interval velocity value of 3000 m s^{-1} was used (Fig. 2, Table 1); for unit B we used the interval velocity of the deeper marine facies (3400 m s^{-1}), which occupies most of the study area. Correction for the effects of compaction was not applied. Although some of the interval velocities used here for depth conversion are approximate we consider them sufficiently adequate for the large scale and scope of the study.

The crystalline basement

The deepest seismic horizon interpreted in this study is the near top of the crystalline basement. It is correlated throughout the study area with the transition from a chaotic and reflection-free seismic character below to a continuous, parallel to divergent, high-amplitude reflections

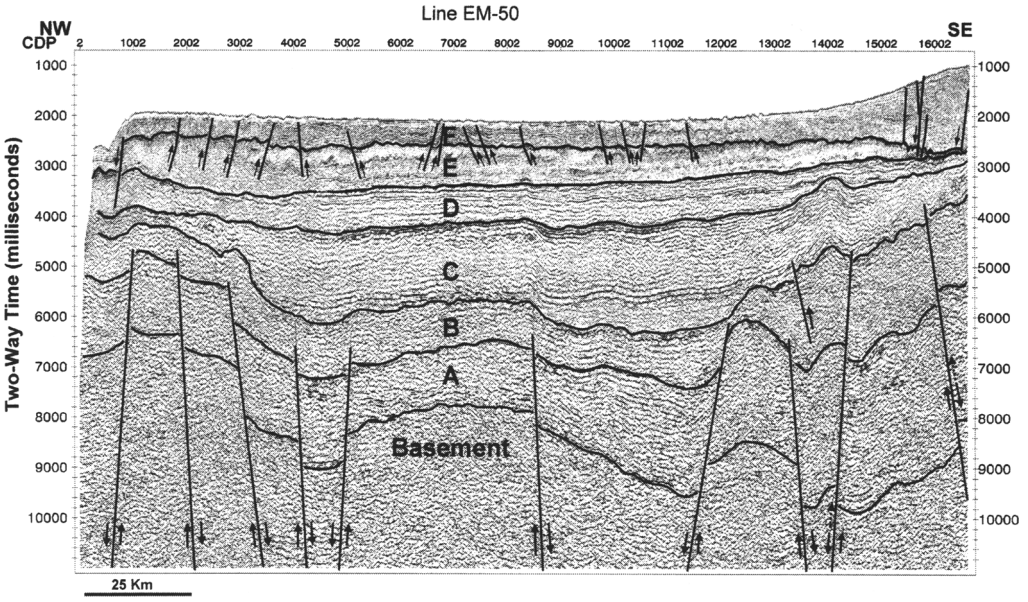

Fig. 3. Interpreted, time-migrated seismic reflection line EM-50 showing the deep structure in the central part of the Levantine basin. A series of normal faults offset the top of the basement, supersequence A and the lower part of supersequence B. Supersequences C–F are not affected by normal faulting. The graben and horst system in the lower part of the basin-fill developed during the Early Mesozoic, Neotethyan rifting phase. Thickness variations in supersequence A (Permian–Aalenian) indicate syntectonic deposition. Fault activity ceased during the deposition of the lower part of supersequence B (Bajocian–Bathonian). Some of the normal faults at the eastern margin of the basin (east of CDP 14000) were later reactivated in a reverse sense of motion during the Syrian Arc contractional phase. The shallow fault system at the top of supersequence E (Messinian evaporites) associated with Plio-Pleistocene halokinesis should also be noted. The location of the profile is shown in Figure 1b.

series above (Fig. 2). We interpret this transition to characterize a major acoustic boundary between non-layered, magmatic and metamorphic basement complexes to the overlying, layered Palaeozoic–Mesozoic sedimentary interval.

The transition in seismic character is more evident in the southeastern corner of the study area, near the Yam West-1 well, where it is found at a relatively shallow depth of about 5–6 s TWT (Fig. 2). In this area the seismic boundary is correlated with the top of the Precambrian to Infra-Cambrian basement penetrated by the Heletz Deep-1 and the Gevim-2 wells (Fig. 1b). The resolution of the seismic data generally decreases below 7–8 s as a result of the reduction of the seismic energy. However, the transition between chaotic seismic character and overlying high-amplitude, partly continuous reflection series was identified below 8 s in many seismic profiles located in the central, deep part of the basin (Figs 3 and 4).

The basement dips gradually westwards from 7 km depth at the Levant shoreline to 14–16 km at the centre of the basin (Figs 5 and 8), and it rises to 5–6 km beneath the Eratosthenes Seamount further NW (Fig. 3; Makris & Wang 1994; Garfunkel 1998; Ben-Avraham *et al.* 2002). The top of the basement marker is dissected by many faults. These are predominantly normal faults in the western and central parts of the basin and reverse faults at the eastern margin (Figs 3–5). Most of the normal faults in the central part of the basin trend to the NE, forming an extensive graben and horst structure extending across the entire basin, from the Eratosthenes Seamount area in the west to the base of the Israeli continental shelf in the east (Fig. 8a).

An 80–100 km wide graben was identified at the centre of the basin where the top of the basement marker reaches its maximal depth (Fig. 8a). This central graben appears to terminate gradually to the NE, across the postulated seaward extensions of the Carmel fault and the Mount Carmel and western Galilee structures (Fig. 8a). No indication was found of a structural discontinuity along these features, as suggested by Ben-Avraham & Grasso (1991) and Ben-Avraham & Tibor (1994). A horst of 15–30 km

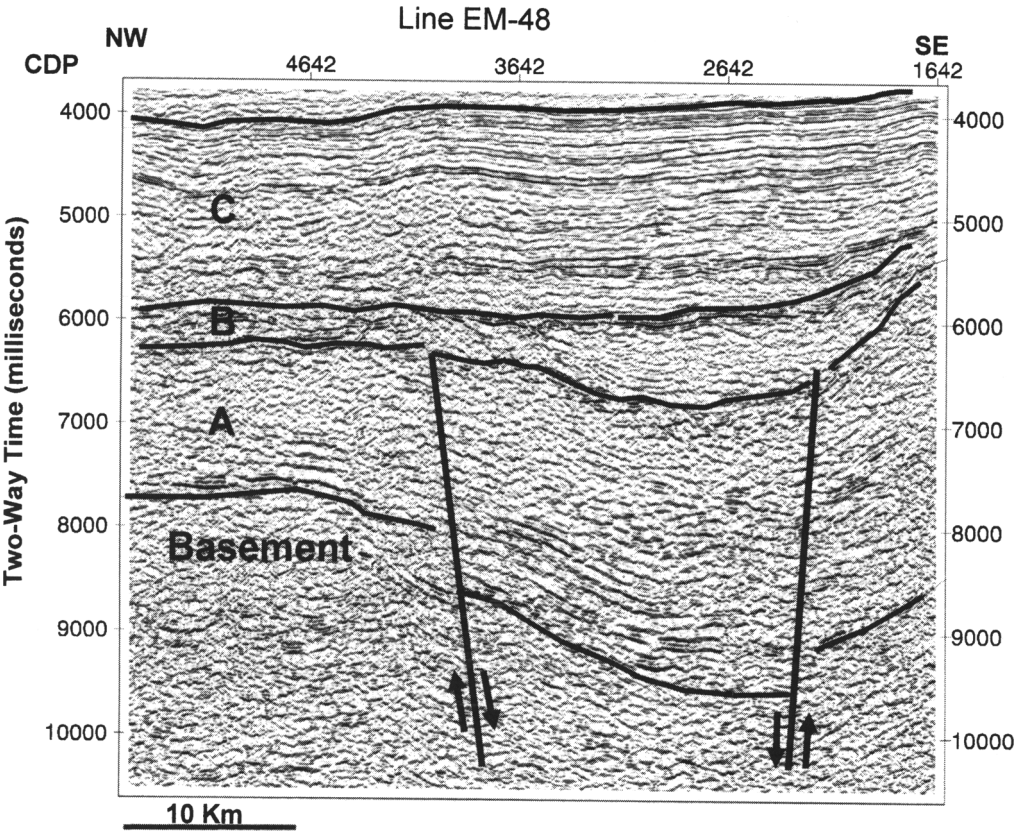

Fig. 4. Interpreted, time-migrated seismic reflection line EM-48 (central part), showing a deep-seated asymmetrical graben in the northern part of the Levantine basin. The graben is interpreted as a Neotethyan rift structure that was formed during the deposition of supersequence A (Permian–Aalenian). The chaotic strata of supersequence B on top of the graben (between CDP 2642 and 3642) are interpreted as post-rift clastic fill. The transition in seismic character from the chaotic crystalline basement to the continuous, high-amplitude parallel reflections in the lower part of supersequence A should be noted. The location of the profile is shown in Figure 1b.

width and 80 km length trending in a NE–SW direction is located in the centre of the graben, where the top of the basement is 2–3 km higher than in the adjacent flanks (Fig. 8a).

Seismic refraction, gravity and magnetic data show that the crust underlying the area of Jordan and Israel thins from 35 km on land to about 10 km within the basin, and that it thickens to about 25 km further west beneath the Eratosthenes Seamount (Ginzburg *et al.* 1979; Makris *et al.* 1983; El-Isa *et al.* 1987; Ginzburg & Ben-Avraham 1987; Makris & Wang 1994; Ben-Avraham *et al.* 2002). The thick crust underneath Israel and the Eratosthenes Seamount is composed of a high-velocity layer at the bottom (6.7 km s^{-1}), and a low-velocity layer on top (6.0 km s^{-1}), interpreted as upper continental crust (Makris *et al.* 1983; Ben-Avraham *et al.* 2002). The absence of the low-velocity layer and the presence of high-velocity (6.7 km s^{-1}), thinned lithosphere in the centre of the Levantine basin was interpreted as an indication of oceanic crust (Ben-Avraham *et al.* 2002). This type of crust is assumed to have been emplaced during Early Mesozoic sea-floor spreading as proposed by the 'oceanic' model.

The nature of the upper crust below the near-top of the basement horizon cannot be directly determined from our seismic data; however, indirect criteria and a comparison with other passive continental margin were used to address the important issue of the crustal composition beneath the Levantine margin and basin.

At the Atlantic continental margin of the USA, the transition between the continental

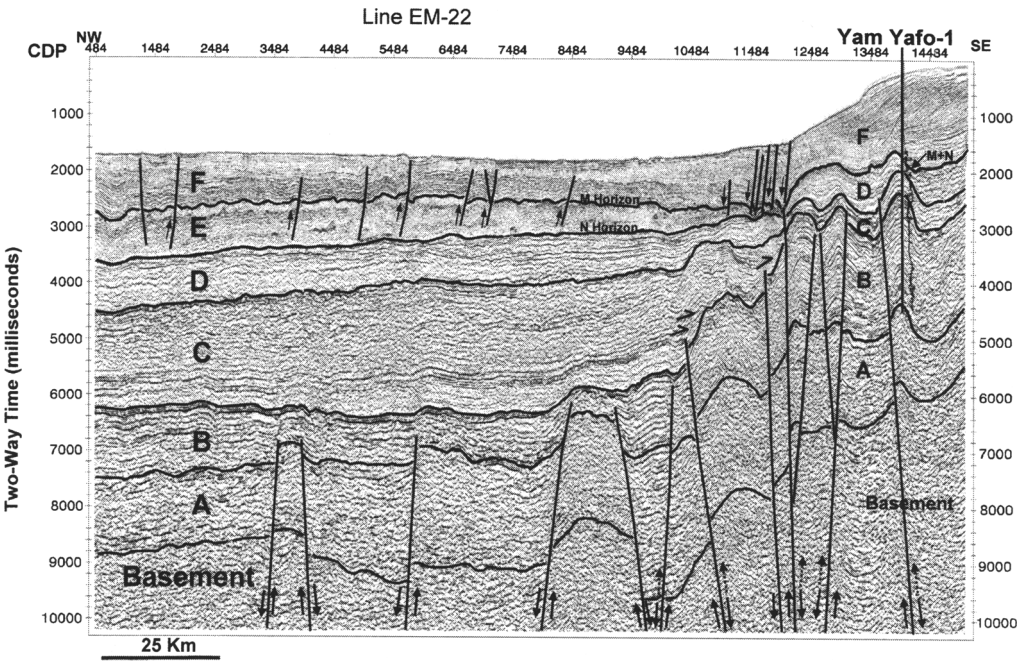

Fig. 5. Interpreted, time-migrated seismic reflection line EM-22 showing the structure of the central and eastern parts of the Levantine basin. An elevated, highly deformed fold belt on the east side of the profile is the western edge of the regional, Syrian Arc fold system that developed in association with the closure of Neotethys. The Syrian Arc contractional deformation started during the deposition of supersequence C (Senonian–Early Oligocene) and ceased during the end of supersequence D (Late Miocene). The reverse, high-angle thrust faults within the fold belt are interpreted as reactivated normal faults of the Early Mesozoic rifting phase. The same type of faults remained inactive in the central part of the basin (west of CDP 10484). The onlapping reflections on the lower boundary of supersequence C (between CDP 9484 and 12484) and the increased thickness of the unit west of the elevated fold belt are associated with drowning of the Mid-Cretaceous shelf coupled with intense transport of clastic material into the basin. The location of the profile is shown in Figure 1b.

crust in the west and the oceanic crust in the east is gradual and takes place through several intermediate zones with distinct physical properties and seismic character, ranging from continental, to rifted, to marginal oceanic and to oceanic (Klitgord & Hutchinson 1988). In our dataset, the basement layer shows similar seismic character across the entire Levantine basin and margin, and no indication for crustal zonation was observed (Figs 3 and 5). Additionally, in the centre of the basin the top of the basement layer does not show the hummocky or mounded character that often characterizes an oceanic basement in the Atlantic margin (Klitgord & Hutchinson 1988) or more locally, in the Ionian Sea at the centre of the Mediterranean Sea (Finetti 1985; Avedik *et al.* 1995).

The deep-seated fault blocks, graben and horsts found throughout the Levantine basin are typical of a rifted or transitional-type crust such as found in the western part of the Atlantic passive margin (Klitgord & Hutchinson 1988). Old rift-related structures would not have been present within new oceanic crust that presumably developed after the main rifting phase. It is therefore suggested, following Hirsch *et al.* (1995), that the basement of the Levantine basin is not oceanic in composition, but rather is a stretched, thinned and probably highly intruded continental crust. The velocity of 6.7 km s^{-1} found in seismic refraction studies is compatible with this type of crust (Hirsch *et al.* 1995). Other supporting evidence for a 'continental' model is the absence of linear magnetic anomalies and the extremely thick sedimentary cover (14–16 km) in the centre of the basin (Hirsch *et al.* 1995). It is assumed that the basement of the Levantine basin has not gone beyond the early magmatic phase of rifting and did not reach full-scale oceanic sea-floor spreading.

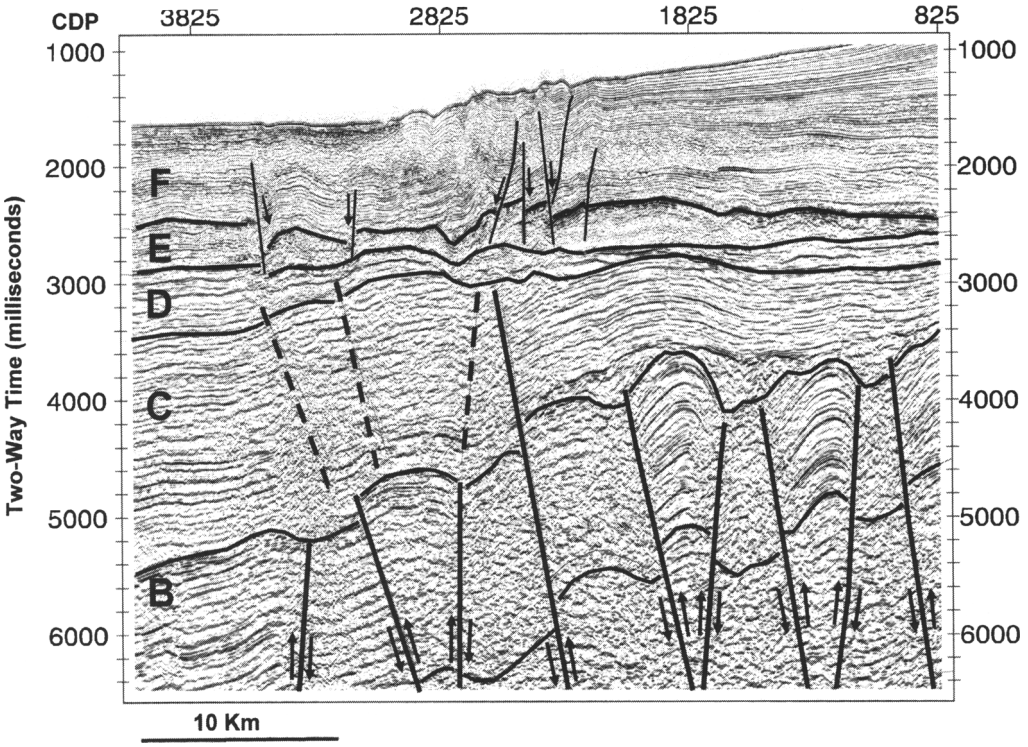

Fig. 6. Interpreted, time-migrated seismic reflection line EM-60 (eastern part) showing contractional deformation at the western edge of the Syrian Arc fold belt. Two folding episodes are observed: an early episode that affected only the strata of supersequence B resulted in high-amplitude, narrow folds and thrust faults (eastern part of the line below 3600 ms); a later episode that affected also the strata of supersequences C and D (eastern part of the line between 3600 and 2800 ms) produced lower-amplitude, wider folds and minor thrusting. Chaotic seismic packages filling the relief in the lower part of supersequence C (near CDP 1825) are interpreted as clastic-rich deposits that were transported into the basin during the early stage of drowning. Shallow, normal faults and folds within supersequences E and F are associated with Plio-Pleistocene halokinesis. The location of the line is shown in Figure 1b.

The Permian to Aalenian supersequence (A)

Supersequence A is a 3–8 km thick unit (1–3s TWT) extending across the entire width of the Levantine basin (Figs 3 and 7a). In the seismic data it is characterized by high-amplitude, relatively continuous, parallel to divergent reflections, locally changing to less reflective or reflection-free zones (Fig. 2). The disruption of seismic character commonly takes place in areas where the unit is highly deformed by normal and reverse faults (Figs 3 and 5).

The lower boundary of supersequence A is the postulated near-top of the crystalline basement. The upper boundary is correlated with a distinct change in seismic character from high-amplitude, continuous reflection series below to discontinuous, low-amplitude, occasionally shingled, reflections above (Fig. 2 at 4500 ms between the Yam-2 and Yam West-1 wells). The change in seismic character is most evident in the eastern part of the basin; however, it is also observed in its central and western parts, where the top of supersequence A is a relatively continuous high-amplitude seismic event below less continuous and lower amplitude reflections (Figs 3 and 5).

Well data indicate that the change in seismic character at the top of supersequence A corresponds to a significant transition in lithology and depositional environment. The continuous, parallel reflections in the upper part of the unit (Fig. 2) are interpreted as shallow-water deposits, probably similar to Triassic and Lower Jurassic platform carbonate found in various onshore wells on the eastern margin of the basin. The

Table 1. *Seismic interval velocities of the basin-fill units (calculated from check shot surveys) in the wells of the study area*

Well names and abbreviations	T.D. (m)	Interval velocities (m s^{-1})				
		Sequence F	Sequence E	Sequences C+D	Sequence B	Sequence A
Asher Yam-1 (AY1)	2020	1921			4865*†	
Ashkelon-2 (As2)	4076					
Atlit-1 (At1)	6531					
Bravo-1(B1)	4096	1750‡		2764‡		
Caesarea-3 (C3)	4600				5077*†	
Delta-1(D1)	4423					
Foxtrot-1 (F1)	2153					
Gaash-2 (Ga2)	5508				5630*†	5990†
Gevim-1 (Ge1)	4620					5800†
Heletz Deep-1(HD1)	6093					5911†
Hof Ashdod-1 (HA1)	3152	2013		3700*	4660*§	
Item-1 (I1)	3708					
Nisanit-1 (N1)	3750				3348*§	
Yam West-1 (YW1)	5250	1660		2539*	2956*§	4494†
Yam Yafo-1 (YY1)	5787	1794		2865	3197§	
Yam-2 (Y2)	5377	1863	3311	2961	2765§	
Average values used for depth conversion		1800	4200	3000	3400	5500

*Shelf facies.
†Incomplete section.
‡Estimated from wireline logs and seismic data.
§Basinal facies.
T.D., total depth.
The interval velocity values were used for depth conversion of interpreted, two-way travel time grids and the construction of isopach and depth maps.

overlying discontinuous, low-amplitude reflections of supersequence B correspond in the offshore, Yam-2, Yam West-1 and Yam Yafo-1 wells to a series of shale, marl, redeposited limestone and some sandstone of Bajocian to Bathonian age. These sediments accumulated in a slope and deep-water environment, basinward of the Mid-Jurassic shallow water carbonate platform (Derin *et al.* 1990; Druckman *et al.* 1994; Gardosh 2002).

The seismic boundary at the top of supersequence A is interpreted as a regional unconformity surface between the Triassic–Lower Jurassic shallow-marine section and the overlying Middle Jurassic deeper marine section. This unconformity is recognized in deep wells at the eastern margin of the basin, where the entire Jurassic section was penetrated. In the onshore Helez Deep-1, Gaash-2, Nissanit-1, Gevim-1, Caesarea-3 and Atlit-1 wells (Fig. 1b), a lithological and biostratigraphic break is identified at the top of limestone and dolomite series (Qeren Formation) of Aalenian age (Hirsch *et al.* 1998). The shallow marine carbonate is overlain by a thin shale and siltstone bed (Rosh Pina Formation) interpreted as a regressive unit (Derin 1974; Hirsch *et al.* 1998). Hirsch *et al.* (1998) correlated this terrigenous unit with an Aalenian sea-level drop at the onset of the LZA-1 eustatic cycle (Haq *et al.* 1988). In some onshore seismic profiles the top of the Qeren carbonate appears as a continuous, high-amplitude reflection similar to the upper boundary of supersequence A in the offshore (Profile DS-3072 and Nisanit-1 well, Fig. 1b).

Supersequence A displays significant thickness variations. The presence of asymmetrical grabens indicates syntectonic deposition and continuous activity of deep-seated faults and basement blocks (Figs 3 and 4). The isopach map shows a large trough, some 90 km wide, trending NE–SW in the central part of the basin (Fig. 7a). The trough is up to 8 km thick in its centre and gradually thins to about 3 km towards the east and west. It is superimposed on a deeper graben mapped on the near-top of the basement horizon (see Figs 7a and 8a).

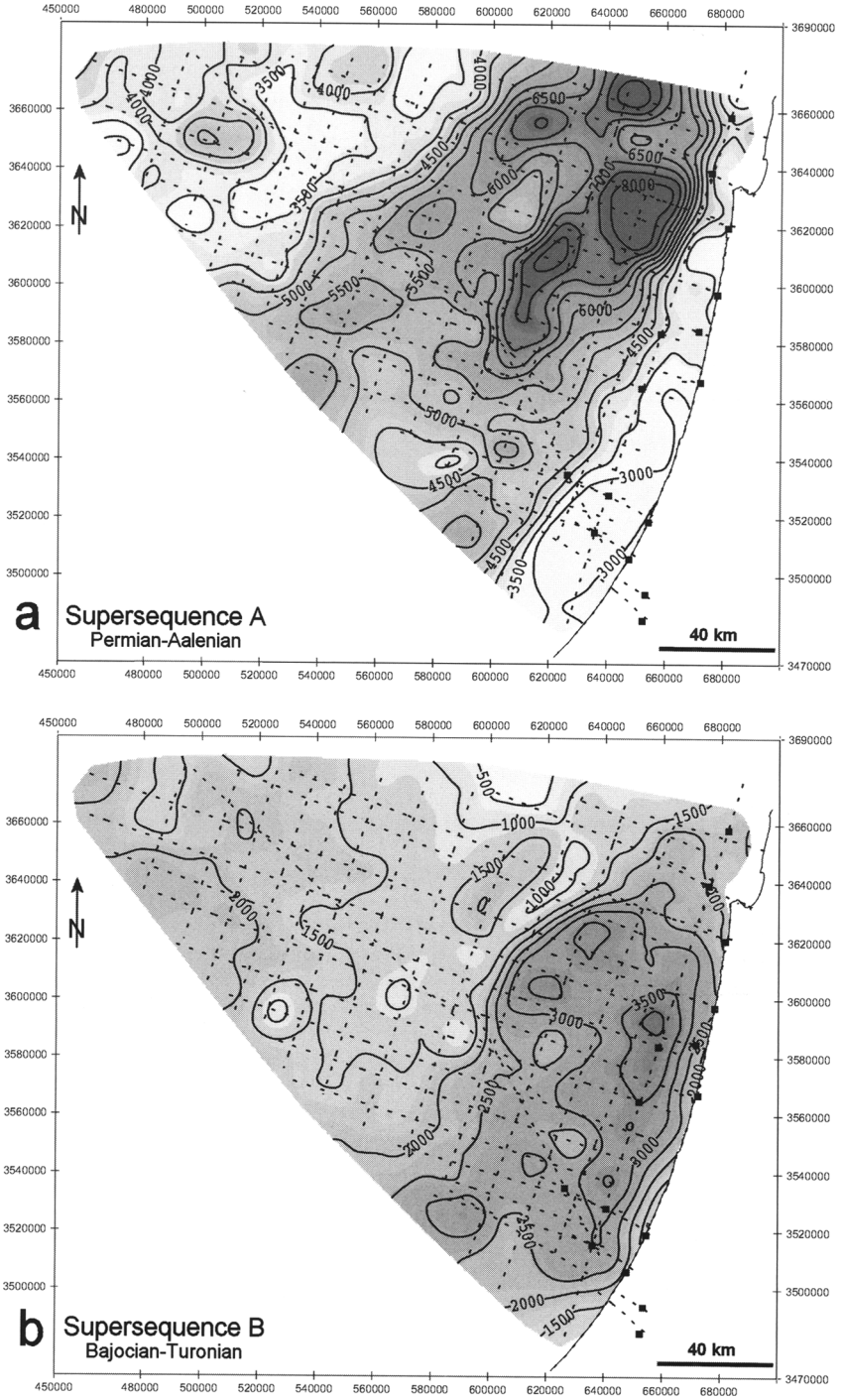

Figs. 7. Isopach maps of the six depositional supersequences composing the Levantine basin-fill. The maps were calculated from two-way travel time grids of the interpreted horizons by using constant, interval velocities (Table 1). (**a**) shows the marked thickness of supersequence A in the centre of the basin (4–8 km) that is associated with syntectonic deposition during the Early Mesozoic, Neotethyan rifting phase. (**b**) demonstrates the eastward shift of depocentre during the post-rift development of the Levantine continental margin.

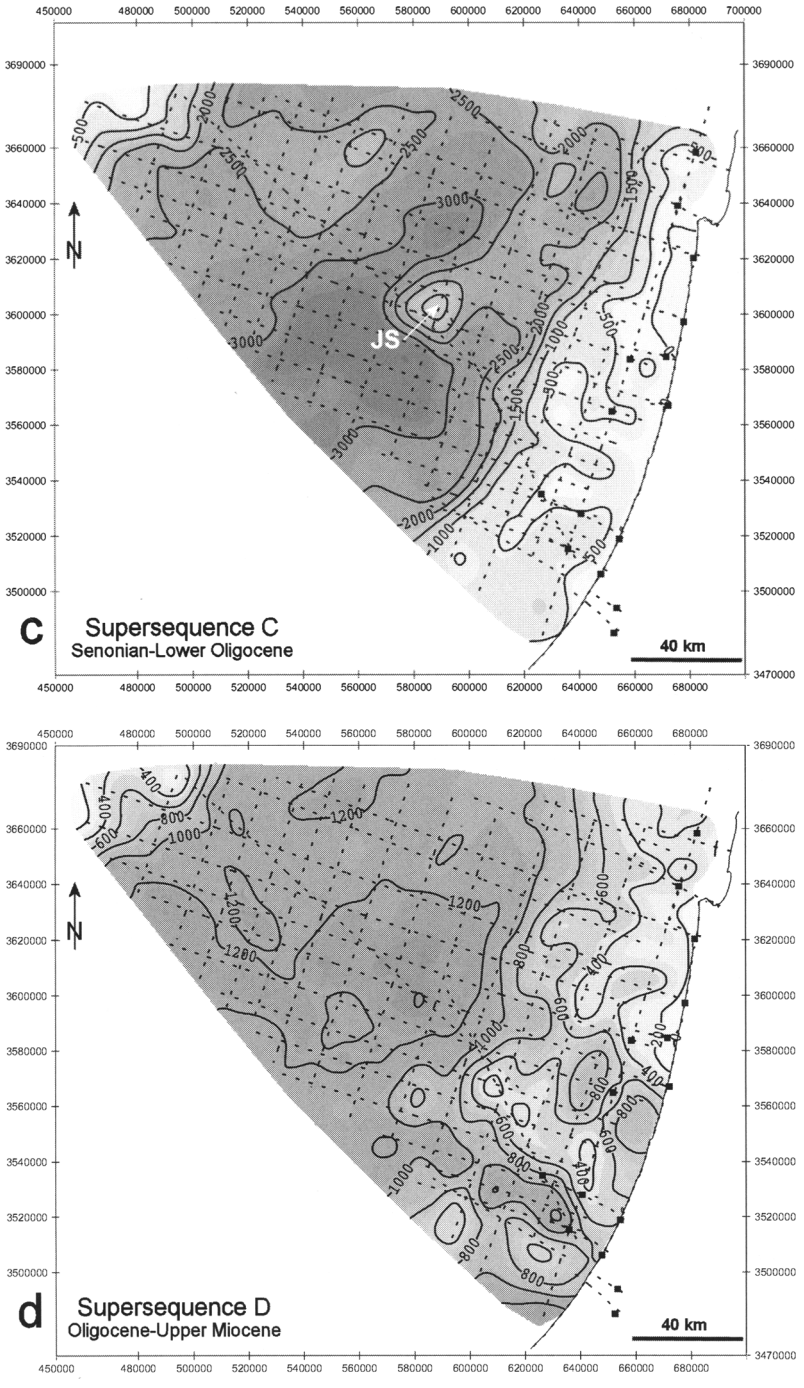

Figs. 7. (**c**) shows the increased thickness of supersequence C in the centre of the basin, probably caused by high influx of clastic material and creation of accommodation within the basin during the Syrian Arc deformation phase. The Jonah Seamount (JS) is interpreted as a Mid-Cretaceous volcanic structure that remained as an elevated submarine high during Senonian to Early Oligocene times. (**d**) shows a more or less equal distribution of supersequence D across the basin with minor thinning towards the eastern margin that reflects the last stage of the Syrian Arc deformation.

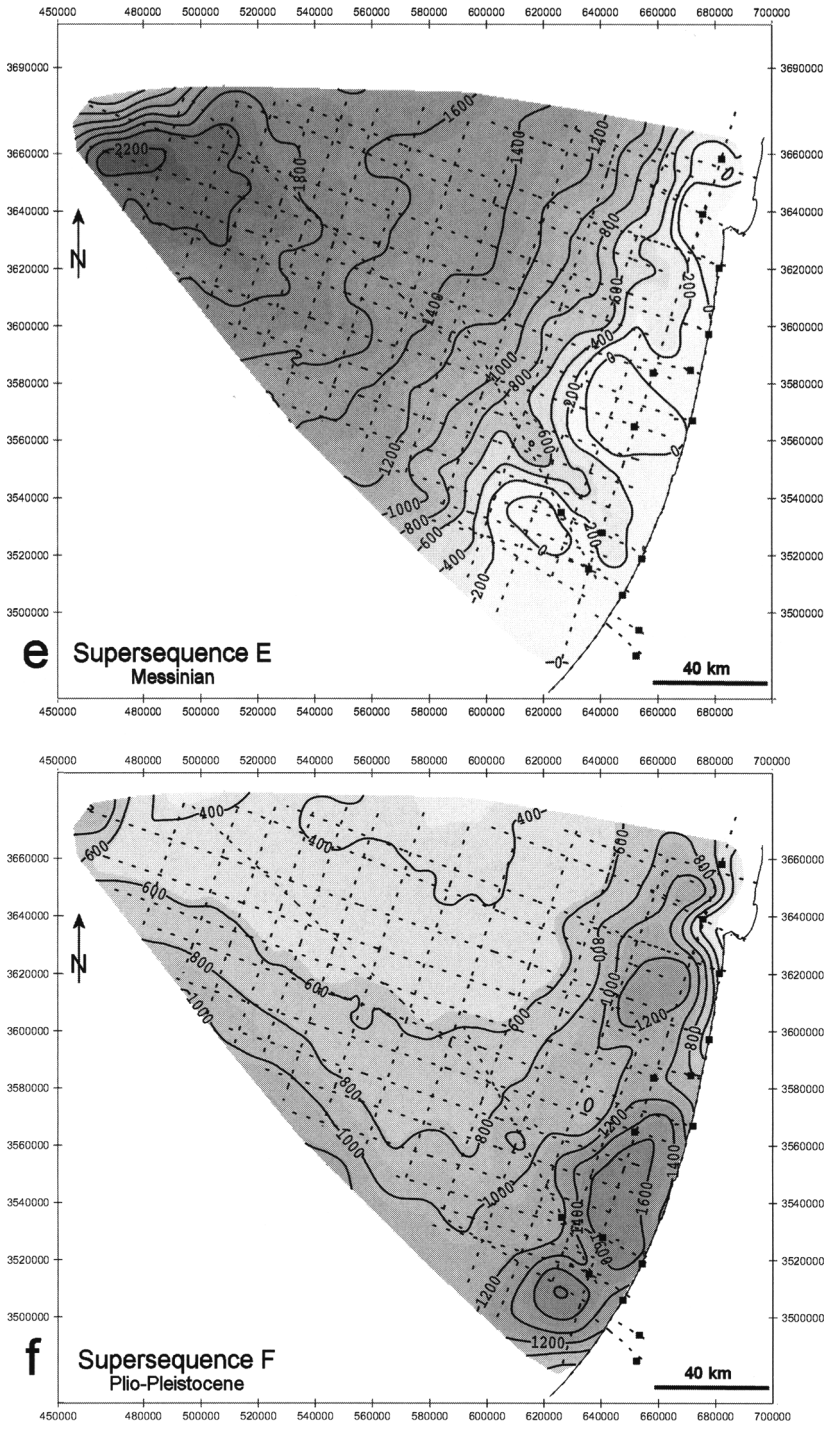

Figs. 7. (**e**) shows the main accumulation of the Messinian evaporite in the centre of the basin and west of the elevated Syrian Arc fold belt. (**f**) demonstrates the thick accumulation of the Plio-Pleistocene prograding sequence along the eastern margin, probably as a result of high influx of both Nilotic and locally derived clastic material.

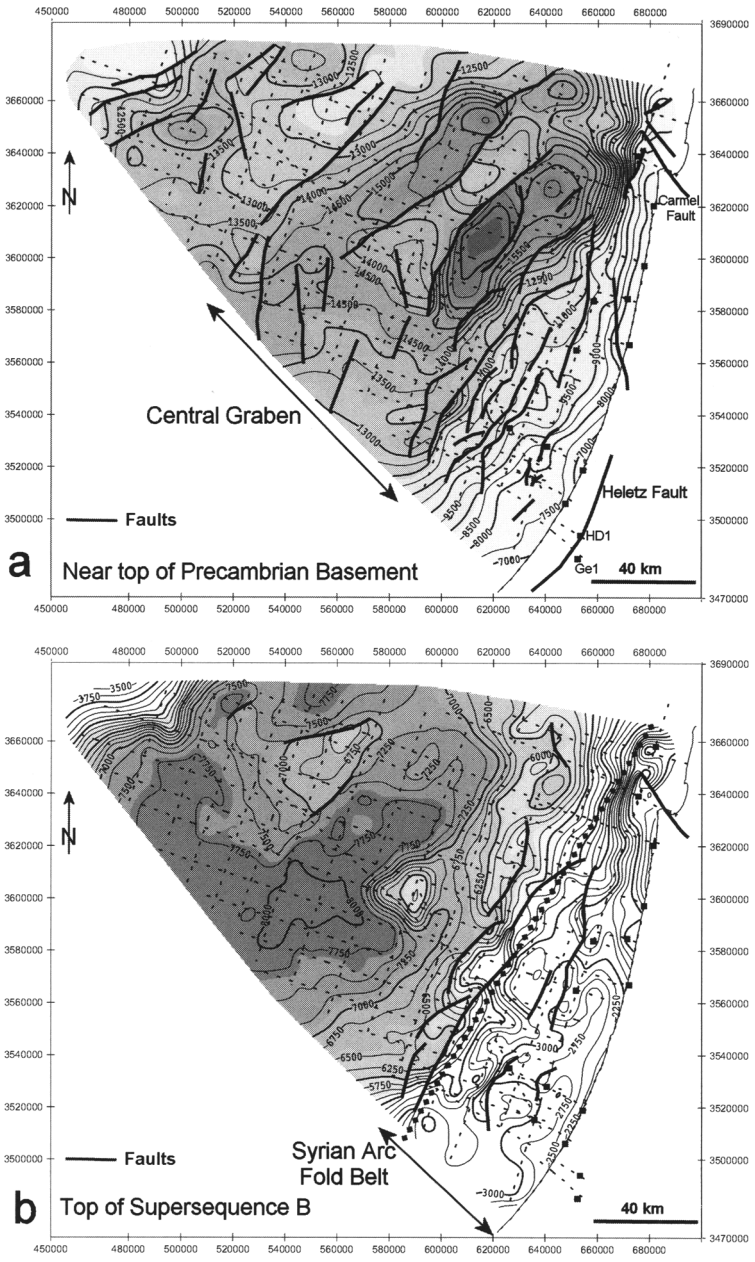

Fig. 8. Structural maps (below MSL) of (**a**) the near-top of the Precambrian basement horizon and (**b**) the top of the supersequence B horizon (Bajocian–Turonian). The near-top basement map shows the extensive SW–NE-oriented normal fault system formed during the Triassic–Jurassic Neotethyan rifting. The most intense rifting took place in the centre of the basin, where the depth to the top of the basement is in the range of 14–17 km. This Central Graben is dissected by an elongated and narrow horst that is possibly associated with intra-rift magmatic activity. The map of the top of supersequence B shows the elevated and highly deformed Syrian Arc fold belt along the eastern margin of the basin. Many of the folds contain high-angle thrust faults. The western edge of the Syrian Arc fold belt follows a zone of crustal discontinuity (dotted line) interpreted from deep refraction and gravity data (after Ben-Avraham *et al.* 2002). It is proposed that the westward termination of the Syrian Arc deformation is related to the deep crustal structure and reflects the transition from a continental crust in the east to a thinned, intruded crust in the west.

Table 2. *The displacement of various stratigraphic markers across the Heletz fault trace, represented by elevations in the hanging wall (Heletz Deep-1) and footwall (Gevim-1)*

Stratigraphic tops in wells	Heletz Deep-1, hanging wall (m below MSL)	Gevim-1, footwall (m below MSL)	Measured vertical displacement (m)	Reconstructed normal throw (m)
Aptian	1069	1555	+486	
Callovian	1783 (reconstructed)	2022	+239	247
Bathonian	1928	2187	+259	227
Bajocian	2724	2494	−230	716
Triassic	4708	3737	−971	1457
Near-top of Infra-Cambrian or Precambrian basement	5714	4460	−1254	1740

The Heletz fault was active in normal motion during the Neotethyan rifting and in a reverse motion during the Syrian Arc contractional phase. The maximal reverse motion, estimated from the displacement of the Aptian level, amounts to 486 m. The normal throw (right column) is reconstructed by adding the reverse motion to the measured vertical displacement of the pre-Aptian units. The total amount of normal throw on the near-top of the Infra-Cambrian or Precambrian basement is 1740 m. A normal throw of 283 m is calculated for the Triassic phase; 741 m is calculated for a Liassic–Bajocian phase, and 489 m for an Early to Mid-Bathonian phase. (For further details see Fig. 9 and the text.)

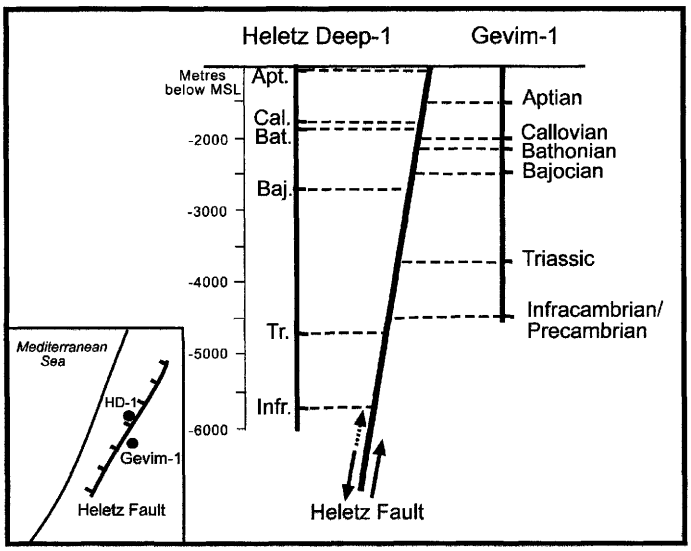

Fig. 9. A schematic geological section across the trace of the Heletz fault, between the Gevim-1 and the Heletz Deep-1 wells. The fault was active in a normal, down-to-the-basin motion during the Neotethyan rifting phase and was reactivated in a reverse motion during the Late Cretaceous, Syrian Arc contractional deformation. Reconstruction of the normal throw on the Triassic and Jurassic stratigraphic levels provides an estimate of the time and amount of displacement during the Neotethyan rifting. (For further details see Table 2 and the text).

The stratigraphy and age of supersequence A within the trough and throughout the Levantine basin are not well established because of lack of well control. Well data from the coastal plain show that Permian sediments overlie the Precambrian basement (Heletz Deep-1, Gevim-1). It is, therefore, assumed that supersequence A is dominated by Permian, Triassic and Lower Jurassic strata. The thickness of this rock section onshore is in the range of 1.5–5 km (Garfunkel 1998), considerably less then the 4–8 km of supersequence A in the offshore (Fig. 7a).

The excessive thickness of supersequence A within the Levantine basin may be partly related to the presence of Palaeozoic or even Infra-Cambrian units that were regionally deposited and later eroded from elevated areas in the nearby continental margin. It is more likely, however, that the main cause of the additional thickness is the syntectonic accumulation of continental, shallow-marine and volcanic rock sections within Triassic and Early Jurassic rift structures.

The occurrence of thick volcanic units in supersequence A is supported by well data from the Haifa area some 40 km eastwards of the main depocentre (Fig. 1b). In the Atlit-1 well Derin *et al.* (1982), Dvorkin & Kohn (1989) and Korngreen (2004) described a Carnian–Norian (Upper Triassic) shallow-water carbonate section of 1141 m thickness, interbedded with 320 m of volcanic rocks. The Triassic sequence is overlain by a 2500 m section of olivine basalts of alkaline affinities known as the Asher Volcanics (Gvirtzman & Steinitz 1983). Argon dating has revealed a mid-Early Jurassic age (193–198 Ma) for the upper part of the volcanic section (Steinitz *et al.* 1983; Kohn *et al.* 1993). The Asher Volcanics do not show mid-ocean ridge basalt (MORB) characteristics and their geochemical signature resembles that of intraplate basalts (Dvorkin & Kohn 1989; Garfunkel 1989). The presence of interbedded shallow-water carbonate, palaeosols and lignites indicates shallow-marine to subaerial volcanism. Garfunkel (1989) proposed that the Asher Volcanics accumulated within a 2–3 km deep, fault-controlled depression in the Haifa area. Similar depressions may have filled with Triassic and Lower Jurassic basalts in the central part of the Levantine basin further west. The existence of thick volcanic units within supersequence A in the offshore is further supported by a strong positive magnetic anomaly over the northeastern part of the basin (Rybakov *et al.* 1997).

In summary, based on the lithological composition found in onshore wells and the seismic character offshore, the strata of supersequence A are interpreted as continental to shallow-marine siliciclastic and carbonate deposits, in places containing thick volcanic sections. The unit was intensely faulted and its deposition took place contemporaneously with extensive rifting and extension throughout the Levant area. No clear evidence was found in the seismic and well data for a deep-marine basin during the Permian to Early Jurassic time span. A shelf break was formed in the Levantine basin only in Mid-Jurassic times, when an aggradational carbonate shelf was established on its eastern margin (Gardosh 2002).

The Bajocian to Turonian supersequence (B)

Supersequence B is an extensive unit attaining its maximal thickness of 3–3.5 km (2–2.5 s TWT) at the eastern margin of the basin (Figs 5 and 7b). Its thickness is reduced to about 1.5 km (1 s TWT) in the central and western parts of the basin (Figs 3, 5 and 7b). In the seismic data the eastern margin area is characterized by a relatively discontinuous, low-amplitude reflection series (Fig. 2, between Yam West-1 and Yam-2 wells), whereas more continuous, high-amplitude reflections characterize the unit in the deep part of the basin, further offshore (Fig. 5).

The lower sequence boundary is correlated with the Middle Jurassic unconformity surface. The upper boundary corresponds to a distinct transition of seismic character between several high-amplitude reflections at the top of the unit and overlying lower-amplitude reflections, marked by chaotic and reflection-free zones (Figs 2, 5 and 6). The upper boundary is evident throughout the deep part of the basin, where the high-amplitude package at the top of supersequence B is particularly continuous and is less disturbed by faulting (see left part of Fig. 5 at 6200 ms). In the eastern part of the basin the sequence is highly folded and its top is characterized by widespread onlapping reflections of supersequence C on the flanks of fold structures (Fig. 2, line EM-24, east of the Yam West-1 well; Fig. 5, the eastern part of line EM-22 between 3000 and 5000 ms).

In the wells of the study area and in outcrops throughout the inland part of Israel the unconformity at the top of supersequence B is indicated by a depositional hiatus; there is a pronounced lithological transition between shelf and slope carbonates of Albian to Turonian age (Judea and Talme Yafe Formations) and pelagic marl and chalk of Senonian to Palaeogene Age (Mount Scopus and Hashefela Groups) (Gvirtzman & Reiss 1965; Flexer 1968; Flexer *et al.* 1986).

The Middle Jurassic to Middle Cretaceous strata comprising supersequence B were penetrated by many onshore and offshore wells in the western part of Israel. An important feature identified in these wells is a pronounced facies change from coarse-grained, shelf-type units east of the present-day coastline to finer-grained, slope and basin-type deposits further west (Derin 1974; Bein & Gvirtzman 1977; Flexer *et al.* 1986). This facies variation indicates the development of a deep-marine basin bordered by a slope and a shallow-marine shelf on the southeastern Levant continental margin (Bein & Gvirtzman 1977).

A detailed sequence stratigraphic analysis of the Middle Jurassic to Middle Cretaceous strata in the southern coastal plain of Israel (Gardosh 2002) shows that the continental margin is composed of six second-order and 22 third-order depositional sequences. These sequences include both lowstand and transgressive to highstand components. The lowstand-type deposits are fine-grained siliciclastic and carbonate debris that was transported into the basin by submarine gravity flows, whereas the transgressive to highstand deposits are coarse-grained bioclastic and siliciclastic deposits that accumulated on the eastern margin in shallow-marine rimmed platforms and ramps (Gardosh 2002). Rapid backstepping and aggradation associated with long-term sea-level rise characterize the carbonate platforms and ramps of the Bajocian–Oxfordian and Cenomanian–Turonian periods. Influx of both siliciclastic and detrital carbonate sediments into the basin was widespread during the Tithonian–Hauterivian and Albian periods.

The steep carbonate shelf edge of supersequence B found near the present shoreline is generally located east of the seismic coverage of the present study. The discontinuous, low-amplitude, occasionally shingled seismic facies of supersequence B in the offshore (Figs 2 and 5) was interpreted as lowstand-type, amalgamated, deep-water turbidite systems composed of siliciclastic and carbonate debris. These kinds of sediments are recognized within the Bajocian–Turonian strata in the Yam Yafo-1, Yam 2 and Yam West-1 wells (Derin *et al.* 1990; Druckman *et al.* 1994; Gardosh 2002). The turbidite flows bypassed the Mid-Jurassic and Mid-Cretaceous carbonate shelves through deeply incised channel and canyon systems. An example of such a channel is the Gevaram canyon, located in the Heletz area of the southern coastal plain (Fig. 1). The canyon is filled with up to 1000 m of Lower Cretaceous (deep marine) shale (Cohen 1976).

Supersequence B reaches a maximum thickness of 2500–3500 m (Fig. 7b). Its depocentre extends from the present coastline to about 50 km westwards, where large amounts of deep-water siliciclastic and carbonate strata accumulated on the upper and lower slopes of the Mid-Jurassic to Turonian margin. Towards the west and near the Eratosthenes Seamount the thickness of supersequence B is reduced to 1000–2000 m (Fig. 7b). It is estimated that in these distal parts of the basin the rate of accumulation of deep-water sediments was considerably smaller. No indication for a shallow-marine carbonate margin is recognized in the Eratosthenes area. Some small, thick accumulations of supersequence B found in the deep offshore are interpreted as localized depocentres filled by clastic material that was eroded and transported from nearby submarine structural highs (note the depression in the eastern part of the line EM-48 between 5500 and 6500 ms in Fig. 4).

The deep-seated normal faults at the centre of the basin affect only the lowermost part of supersequence B (Figs 3–5). At the eastern margin, most of the older, normal faults were later reactivated as thrust faults. Reconstruction of the reverse motion shows a normal displacement in the range of several hundred metres of the Middle–Upper Jurassic to Middle Cretaceous strata. The minor effects of faulting indicate that most of the deposition of supersequence B took place in a post-rift stage when the basin was dominated by cooling and thermal subsidence. The termination of this depositional cycle coincides with the onset of large-scale contractional deformation. This tectonic event, known as the Syrian Arc folding phase, is recognized throughout the southern and eastern margins of the Levantine basin, and is associated with the closure of the Neotethys Ocean during the Late Cretaceous to Early Cenozoic, at the time of deposition of supersequence C.

The Senonian to lower Oligocene supersequence (C)

Supersequence C attains its maximal thickness of about 2.5–3 km (2 s TWT) in the central part of the Levantine basin and displays marked thinning towards the eastern and western margins (Figs 3 and 7c). It is generally characterized by low- to medium-amplitude, continuous and parallel reflections, chaotic reflections and reflection-free zones (Fig. 2). Well data indicate that this seismic character corresponds to chalk and marl of pelagic to hemipelagic, deep-water origin throughout the basin (Almogi-Labin *et al.* 1993).

Within the basin and on its eastern margin extensive onlapping is observed on the lower boundary of supersequence C (Figs 2 and 5). Similar onlapping of Senonian strata on Cretaceous slope and shelf carbonate (Talme Yafe and Judea Groups) is found in the southern coastal plain (Gardosh 2002). An erosional unconformity associated with subaerial exposure is recognized at the Turonian–Coniacian boundary (base of supersequence C) in outcrops throughout the inland part of Israel (Bentor & Vroman 1960; Flexer 1968). Both erosion and onlapping are interpreted as the result of a relative sea-level drop that was followed by eustatic rise and drowning of the Mid-Cretaceous carbonate platform (supersequence B). The drowning caused

the cessation of the Albian–Turonian carbonate factory on the shallow shelf and the replacement of platform carbonate with Senonian pelagic chalk (Sass & Bein 1982; Almogi-Labin *et al.* 1993; Buchbinder *et al.* 2000).

In the central part of the basin the lower several hundred milliseconds of the supersequence C are characterized by a reflection-free, transparent zone (Figs 4 and 5). In the eastern fold belt chaotic reflection packages are found within deep synclines, overlying supersequence B (the eastern part of line EM-60 between 3500 and 4000 ms in Fig. 6). The transparent to chaotic seismic character at the base of the unit is interpreted as coarser-grained, clastic-rich sediments probably associated with a frequent supply of hemipelagic gravity flows during the early stage of drowning. The top of the chaotic package constitutes, in places, a high-amplitude truncation surface (the eastern part of line EM-60 at 3500 ms in Fig. 6), interpreted as a higher-order sequence boundary within the Senonian to Lower Oligocene supersequence (Gardosh 2002).

The upper boundary of supersequence C is correlated with the top of a relatively continuous higher-amplitude reflection series, in turn overlain by low-amplitude and occasionally mounded reflections (Figs 3 and 5). The change in seismic character corresponds to an unconformity surface in the offshore Yam Yafo-1, and Yam West-1 wells (Fig. 2), as indicated by a pronounced lithological break and a biostratigraphic hiatus between Middle Eocene carbonates and an overlying section of Oligocene to Miocene siliciclastic deposits (the Saqiye Group; Druckman *et al.* 1994; Gill *et al.* 1995).

On the isopach map supersequence C displays an almost symmetrical thinning pattern, from 3000 m in the central part of the basin to <500 m on both its eastern and western margins (Fig. 7c). An exception to this pattern is a prominent elevated structure located in the centre of the basin where the unit is only 1500 m thick (Fig. 7c). This feature was termed the Jonah Seamount and interpreted by Folkman & Ben-Gai (2004) as an intrusive structure of Oligo-Miocene age. An Oligo-Miocene age for the Jonah Seamount is not supported by the present data, as the structure is not observed on the isopach map of supersequence D (Fig. 7d). An alternative interpretation suggests reduced deposition of Senonian to Early Oligocene strata over a pre-existing submarine high, shown as a prominent structure in the centre of the basin on top of supersequence B (Fig. 8b). The Jonah Seamount is interpreted as a volcanic structure of Mid-Cretaceous age. Relevant volcanic phases are known to have occurred in the area during the Albian and Cenomanian (Garfunkel 1989). The reduced section overlying this high (supersequence C) may have been deposited as a carbonate build-up or an atoll.

Calculated sedimentation rates in the central part of the basin are in the range of 33–50 m Ma^{-1} (uncorrected for compaction), but along the margin only about 8 m Ma^{-1}. The low rate of deposition in the margin is similar to rates reported by Buchbinder *et al.* (1988) for undisturbed Eocene chalk in outcrops further onshore. The great thickness and high rate of sedimentation, as well as the widespread onlapping and the chaotic seismic character in the lower part of the unit are all indicative of significant gravity transport and influx of clastic sediments into the basin. These processes are associated with the creation of accommodation space probably through both tectonic subsidence and relative sea-level rise during the time of deposition of supersequence C.

The Oligocene to upper Miocene Supersequence (D)

Supersequence D is 0.5–1 km thick unit (0.3–0.7 s TWT), extending across the entire width of the basin (Fig. 7d). In the seismic profiles it is characterized by low-amplitude, partly discontinuous reflections, some mounded reflections and reflection-free zones (Fig. 2). The lower sequence boundary is the base Oligo-Miocene unconformity (base Saqiye siliciclastic rocks). The upper boundary is correlated in the central part of the basin with a marked transition in seismic character between the reflection series of supersequence D and the chaotic and reflection-free seismic package of the overlying Messinian evaporites (supersequence E) (Figs 3, 5 and 6). In the eastern part of the basin, where Messinian evaporites are either thin or missing, the upper sequence boundary corresponds to a conspicuous surface of erosional unconformity and a biostratigraphic hiatus, as recognized in both well and seismic data at the base of the Plio-Pleistocene section (Yafo Formation) (Gvirtzman & Buchbinder 1978; Druckman *et al.* 1995).

In the offshore Yam West-1 and Yam Yafo-1 wells (Fig. 1b), supersequence D is composed of pelagic marl and shale of Oligocene to Late Miocene age (Lower Saqiye Group) (Druckman *et al.* 1994; Gill *et al.* 1995). Thick intervals of coarse-grained sandstone and conglomerate were found onshore within the sequence in wells along the eastern margin (e.g. Hof Ashdod-1, Fig. 1b). These sediments are interpreted as canyon-fill deposits associated with several

cycles of subaerial and submarine erosion and incision on the Oligo-Miocene shelf (Gvirtzman & Buchbinder 1978; Druckman *et al.* 1995; Buchbinder & Zilberman 1997; Buchbinder & Siman Tov 2000).

Mounded reflections identified within supersequence D in the offshore (the eastern part of profile EM-60 at 2800 ms in Fig. 6), are interpreted as siliciclastic, deep-water turbidite systems and basin-floor fans. These may be the distal equivalents of the proximal canyon-fill deposits found onshore. The presence of coarser-grained siliciclastic material within the fine-grained strata of supersequence D may explain the overall low-amplitude and discontinuous seismic character of the unit in the offshore record (Fig. 5).

The Messinian supersequence (E)

The Messinian sequence is a distinct seismic package identified throughout the eastern Mediterranean region, composed of thick evaporitic series of Late Miocene age (Hsü *et al.* 1973; Neev *et al.* 1976; Ryan 1978). In the Levantine basin this unit is about 1–2 km thick (0.5–1 s TWT), extending across most of the basin (Figs 3 and 7e). The lower and upper boundaries are the well-known seismic markers defined in previous works as the N and M horizons. Supersequence E generally displays a chaotic seismic character that is typical of massive rock salt (Figs 3 and 5). Continuous reflection packages found within the unit are interpreted as anhydrite and shale intercalations such as in the Yam-2 and Yam West-1 wells (Fig. 2).

The area of evaporite accumulation extended throughout the deep part of the basin to about 20–40 km west of the present-day coastline (Fig. 7e). The evaporitic brine was probably limited to the east by a steep slope composed of the topographically higher strata of supersequence D (Fig. 5). However, during highstand episodes the brine covered this slope and penetrated through deep canyons further inland. Remnants of the Messinian brine in the form of halite and anhydrite beds a few tens of metres thick were encountered in various wells in coastal areas of Israel (Druckman *et al.* 1995).

Halokinesis occurs throughout the basin, affecting the salt layer and the overlying Plio-Pleistocene strata up to the sea-bed surface (Figs 3, 5 and 6). In the eastern margin, salt-flow has resulted in the development of normal, occasionally listric faults, whereas in the central and northwestern part of the basin and near the Eratosthenes Seamount the salt layer is affected by many thrust faults and folds (Figs 3 and 5). Gradmann *et al.* (2005) recently suggested that both extension and compression of the Messinian evaporites are associated with thin-skinned salt tectonics related to the subsidence of the basin during post-Messinian time. Basinward creep of the salt layer resulted in normal faulting on the eastern slope and reverse faulting and buckling in the distal part of the basin. A considerable increase of salt thickness towards the western part of the basin may be associated with salt flow in this direction (Figs 3 and 7e).

The Plio-Pleistocene supersequence (F)

The Plio-Pleistocene supersequence attains its maximal thickness of about 1.6 km (1.6 s TWT) along the eastern margin and it is reduced to several hundred metres in the central part of the basin and towards the Eratosthenes Seamount (Figs 3 and 7f).

The upper sequence boundary is the sea bed. The lower boundary is a composite unconformity surface. Within the basin this boundary corresponds to the top of the Messinian evaporites (M horizon). In the eastern margin, where the evaporites are missing, the M and N horizons merge and the composite surface coincides with the base Messinian unconformity (Fig. 5). In other parts of the Mediterranean region, this surface is marked by a short lived post-evaporitic fluvial and euryhaline episode that predated the establishment of Pliocene normal, deep-marine conditions, known as the Lago Mare event (Hsü *et al.* 1978; Rouchy & Saint Martin 1992).

Throughout the basin, the sequence is characterized by continuous, thin high- and low-amplitude reflections. In the central part, these are highly deformed as a result of underlying salt flow. At the eastern Levantine margin, where the unit attains its maximal thickness, it is dominated by sigmoidal progradational reflection patterns (Figs 2 and 5). Well data show that the Plio-Pleistocene section, termed the Yafo Formation, is a mud-dominated unit composed mostly of claystone and siltstone (Gvirtzman & Buchbinder 1978) (see Yam West-1, Fig. 2). Isolated, coarser-grained sand bodies containing large amounts of biogenic gas were recently found within submarine channels and basin-floor fans in the lower part of the supersequence, south of the Yam West-1 well (Fig. 1b).

The depositional mechanisms of the fine-grained clastic material composing the Plio-Pleistocene supersequence F are not yet adequately studied. Part of the material was probably transported through longshore currents from the Nile cone located about 200 km to the SW (Fig. 1) (Gvirtzman & Buchbinder 1978; Ben-Gai

1996). Several lines of evidence suggest an additional local source to the east and SE. First, the conspicuous sigmoidal, progradational reflection pattern is oriented perpendicular to the present-day coastline, thus suggesting transport from exposed land to the east. Second, the unit attains its maximal thickness along the eastern coast, and only a minor increase in thickness towards the SW is observed (Fig. 7f). Third, a NW–SE-oriented canyon and channel systems of Late Cenozoic age was identified in well outcrop and seismic data from the southern coastal plain of Israel (Afiq, Ashdod and Gaza canyons) (Gvirtzman & Buchbinder 1978; Druckman *et al.* 1995). These canyons were probably preferred conduits for submarine turbidite flows and basinward transport of clastic material supplied from a subaerial drainage system to the east and SE.

It is suggested that during the time of deposition of supersequence F (Plio-Pleistocene) topset-clinoform systems composed of large shelf-edge deltas prograded along the Mediterranean coastline. Huge amounts of fine-grained siliciclastic sediments accumulated at the mouth of submarine canyons and channels. The great thickness of the unit west of the present coastline (Fig. 7f) is associated with particularly high sedimentation rates of about 300 m Ma^{-1}. The rate of supply exceeded the rate of accommodation space, thus resulting in progradation of the shelf break to *c.* 20 km basinwards (at the top of line EM-22 near the Yam Yafo-1 well; see Fig. 5). The intensity of the depositional processes is associated with the combined effects of global and local factors. These include a rapid rise of Pliocene sea level, subsidence within the basin as a result of sediment loading of the Nile cone, and the uplift of the Judea and Samaria mountain range located 20–50 km east of the basin.

Discussion

Tectonic evolution

The mapping of the near-top Precambrian basement (base of supersequence A) (Fig. 8a) and top-Turonian surfaces (top of supersequence B) (Fig. 8b) reveals two important deformation phases of the Levantine basin and margin. An early, extensional phase caused normal faulting of the basement and the overlying Palaeozoic to Early Mesozoic strata. A later, contractional phase resulted in reverse faulting and folding and the formation of the Syrian Arc mountain range. The first phase is related to Early Mesozoic rifting that led to the separation of the African–Arabian and Eurasian plates and the opening of Neotethys. The second phase is associated with Late Mesozoic convergence and subduction that accompanied the closing of the Neotethys ocean system. Extensive evidence for the two deformation phases was previously found in outcrops and boreholes throughout the Levant region onshore (see Garfunkel 1998, 2004). Additional evidence for these events is presented here for the offshore Levantine basin.

Neotethyan rifting phase

Within the study area, the eastern Mediterranean basin consists of a series of deep-seated, tilted fault blocks downfaulted from its margins (Israeli coastline and the Eratosthenes Seamount) towards its centre. The geometry of this fault system is recognized in the western and central parts of the basin where deep structures are well imaged. In this area the faults can be traced over long distances and extend from a few kilometres to several tens of kilometres (Fig. 8a). The spacing between the faults is in the range of 5–20 km and some of the blocks are asymmetrical half-grabens (Figs 2–4).

The normal faults were active during the time span of supersequence A (Permian–Aalenian), dying out towards the top of the unit, or in some areas affecting the lower part of supersequence B (Bajocian–Turonian) (Figs 2–5). The vertical displacement on these faults is seen on the top of the basement horizon in the central and western parts of the basin, where it ranges from several hundred metres to 2–3 km (Fig. 8a).

In the area east of the Eratosthenes Seamount normal faulting during the deposition of supersequence A accounts for almost the entire structural relief on top of the basement structural map (Figs 3 and 8a). On the eastern margin of the basin most of the deep-seated faults were inverted in the Senonian–Miocene and it is difficult to measure their original vertical displacement. However, thickness changes of supersequence A across some of the faults indicate downfaulting of at least a few hundred metres during the early, rifting phase. Unlike the western margin of the basin, normal faulting during supersequence A accounts only for half of the 8–10 km relief on top of the basement on the eastern margin (see line EM-22 in Fig. 5 and the isochore map in Fig. 7a).

The amount and timing of vertical displacement in the eastern Levant margin are more accurately estimated from the subsurface of central and southern Israel. In this area, seismic and well data show evidence for considerable down-to-the-basin normal faulting in the Triassic and Jurassic section (Druckman 1977, 1984; Gelberman & Kemmis 1987; Garfunkel 1989, 1998; Cohen

et al. 1990; Druckman *et al.* 1995). An example of such a displacement is recorded on the Heletz Fault (Figs 8a and 9). This major, NE–SW-trending normal fault was mapped in the subsurface of the southern coastal plain of Israel by Gelberman (1995). A comparison of the depth of different stratigraphic markers found in the Gevim-1 well on the footwall, and the Heletz Deep-1 well on the hanging wall allows quantification of the history of motion (Table 2, Fig. 9).

The Heletz fault was active in a down-to-the-basin, normal sense during the Neotethyan rifting phase and was reactivated in a reverse motion during the Late Cretaceous Syrian Arc contractional phase. The amount of reverse motion on the hanging wall of the fault can be estimated from the 486m displacement of the top-Aptian level (Table 2, Fig. 9). The normal throw of the deeper stratigraphic levels is calculated by adding the reverse motion to the measured vertical displacement (Table 2). The total, reconstructed normal throw of the near-top of the Precambrian basement is 1740 m. The vertical motion during the Triassic phase amounts to 283 m; this probably took place mainly during the Anisian and Carnian (Table 2) (Druckman 1984). A vertical motion of 741 m is calculated for a Liassic–Bajocian phase and 489 m for an Early to Mid-Bathonian phase (Table 2). Increased thickness of the Triassic to Bathonian strata on the hanging wall of the Heletz Fault indicates syntectonic deposition (Fig. 9). The top-Bathonian and the reconstructed top-Callovian levels are similarly displaced (227 m and 247 m, respectively) suggesting some additional, post-Mid-Jurassic tectonic activity (Table 2).

The Heletz Fault provides direct evidence for the activity of the Neotethyan rift system in the Levantine basin during the Mid-Triassic (Anisian), Early and Mid-Jurassic (Liassic–Bathonian). Rifting may have taken place already in the Permian, as can be inferred from other Neotethyan structures (Palmyra trough; Garfunkel, 1998). However, possible earlier activity in the Levantine basin is speculative because of lack of relevant well data.

The overall thickness of supersequence A within the basin (central graben) is 4–8 km (Fig. 7a). Coeval units found within fault-controlled depressions onshore, such as the interior basin of central Israel and the Palmyra trough of Syria, are only 3–5 km thick (Garfunkel 1998). It is, therefore, concluded that the centre of the Levantine basin was the most active part of the Early Mesozoic, Neotethyan rift system of the Levant area.

The Levantine basin was bounded by the Arabian Massif to the SE and the Eratosthenes continental block to the west. It was thus probably separated from the main body of the Neotethys Ocean that may have extended north of the Eratosthenes Platform and was later consumed underneath Cyprus and southern Turkey (Garfunkel 1998, 2004; Robertson 1998).

An important question regarding the nature of the Neotethyan rifting processes is whether emplacement of new oceanic crust took place in the Levant area. Apart from faulting no pronounced disruption and conspicuous lateral variations in the seismic properties of either the upper part of the basement or supersequence A are observed in our dataset. The basement layer in the central part of the basin does not show any characteristics of oceanic crust such as described in other passive continental margins (Klitgord & Hutchinson 1988) or in the central part of the Mediterranean Sea (Finetti 1985; Avedik *et al.* 1995). The normal faults and basement structures associated with an early rifting stage are well preserved. Although a considerable amount of Triassic and Jurassic volcanic rocks may exist within the basin, their equivalent units in the onshore area (Asher volcanic series) do not show MORB characteristics associated with sea-floor spreading. Thus, the occurrence of spreading and introduction of new oceanic crust as implied by the 'oceanic' models are not supported by the present data.

It is suggested that rifting during the Early Mesozoic was responsible for the significant thinning of the crust in the centre of the Levantine basin. However, rifting, thinning and oceanic physical properties, as interpreted from seismic velocities by Ben-Avraham *et al.* (2002), do not necessarily imply sea-floor spreading. The basin may not have reached the spreading phase as is the case in the northern parts of the Red Sea. There, the rift is continental, with only the nucleation of an oceanic spreading centre and an early magmatic phase. An oceanic spreading centre has come into existence only in the southern and central parts of the Red Sea (Martinez & Cochran 1988; Bohannon & Eittreim 1991; Cochran 2001).

It should be emphasized that the Red Sea model compares well with the Levantine basin in term of physical dimensions and properties, although the duration of the rifting and early magmatic phases are entirely different: 10–15 Ma in the Red Sea and *c.* 75–80 Ma in the eastern Mediterranean.

The general strike of the normal faulting mapped in our study in the Levantine basin is NE–SW. Accordingly, we interpret rifting and extension in a NW–SE direction perpendicular to the strike of the faulting. This interpretation

cannot comply with rifting and spreading of the eastern Mediterranean in a north–south direction, accompanied by a transform fault along the eastern Mediterranean shoreline as proposed by Dewey *et al.* (1973), Bein & Gvirtzman (1977), Robertson & Dixon (1984) and Stampfli *et al.* (2001).

The model of opening in a NW–SE direction and an east–west, strike-slip motion along the northern coast of Sinai, as suggested by Garfunkel & Derin (1984) and Garfunkel (1998) is in good accordance with our data. This model further implies that the eastern Mediterranean rift became detached from a Neotethys spreading centre that existed further north, beyond the northern palaeo-margin of the Arabian Massif.

The passive nature of the eastern Levant margin with its rimmed carbonate shelf was established as early as late Mid- and Late Jurassic (Bathonian–Oxfordian), and persisted until the end of the Turonian (Gardosh 2002). Our data show marked differences between the eastern and western margins of the eastern Mediterranean basin during this time span: the density and dimensions of faulting are different on the two sides (Fig. 8a and b), thick sedimentary depocentres of supersequences A and B are located near the eastern margin but are missing from the western side (Fig. 7a and b), and no distinct passive margin geometry is identified near the Eratosthenes Seamount (Fig. 3). The only shallow-water sediments recorded from the Eratosthenes area are of Miocene age (Mart & Robertson 1998).

Rybakov & Segev (2004) recently questioned the assumed shallow depth and continental nature of the basement underlying the Eratosthenes Seamount. Our dataset reaches only the eastern Eratosthenes and does not permit a comprehensive analysis of this area. A better understanding of the geology of the Eratosthenes Seamount is essential to fully reconstruct the evolution of the eastern Mediterranean basin during Early Mesozoic times.

Syrian Arc inversion and contraction phase

An elevated zone of contractional deformation extending offshore, some 70 km west of the present coastline (Fig. 8b), is interpreted as the subsurface continuation of the 'Syrian Arc' (Krenkel 1924) or 'Levantine' (Horowitz 1979) fold belt. This regional tectonic feature forms a S-shaped mountain belt extending from the Palmyride Mountains in Syria and Lebanon and the Anti-Lebanon Mountains in Lebanon, through the Judea Mountains and Negev anticlines in Israel and into the northern Sinai anticlines in Egypt (Fig. 1) (Picard 1943, 1959; Ball & Ball 1953; Bentor & Vroman 1954, 1960; de Sitter 1962; Gvirtzman 1970; Bartov 1974; Neev *et al.* 1976; Garfunkel 1978; Horowitz 1979; Eyal & Reches 1983; Lovelock 1984; Beydoun 1988; McBride *et al.* 1990). Its extension further SW is masked by the thick Mio-Pliocene sediments of the Nile delta (Aal *et al.* 2000).

In the study area, supersequence B rises some 3500 m from the foot of the Syrian Arc mountain belt in the west to its top near the coastline (Figs 5 and 8b). The dominant deformational style within the fold belt is high-amplitude and short-wave length anticlines and monoclines, underlain by high-angle thrust faults (Figs 5 and 6). Individual structures range from 10 to 30 km in length and from 5 to 10 km in width. Their height ranges from several hundred metres to more than 1000 m, and their flanks dip at 10–30°. The thrust faults dip at 65–75° and can be traced down into the basement and up to the Middle–Upper Cretaceous section.

A second, less widespread style of deformation observed within the contractional belt is of wider folds (up to 15 km) with lower amplitudes of up to several hundred metres. In the eastern margin, these broad and shallow folds are occasionally found superimposed on high-amplitude, narrow folds (Fig. 6). Some low-amplitude folds of the second style of deformation are found also in the deeper basin, west of the Syrian Arc fold belt. The kinematics of these structures is currently not fully understood.

The entire supersequences A, B and C and the lower part of supersequence D are affected by the contractional deformation. Thickness variations and onlapping reflections within supersequences C and D indicate that they were deposited contemporaneously with the folding. Assuming only minor mis-correlations and incorrect dating of our seismic units it is suggested that the contraction phase started in the Late Cretaceous and persisted until the Early–Mid-Miocene (Fig. 5). The folding took place in recurrent episodes, thus resulting in more intensive deformation of the older sections. A similar timing for the onset of folding was suggested from studies of the Syrian Arc (e.g. Bentor & Vroman 1960; Bartov 1974; Beydoun 1988; McBride *et al.* 1990; Garfunkel 1998). However, the time of cessation was previously not well established, mainly because of the lack of relevant field relations.

Compelling evidence for inversion of Early Mesozoic extensional structures during the Late Cretaceous folding phase comes from various parts of the Syrian Arc fold belt in onshore Israel and Syria (Freund *et al.* 1975; Druckman 1981; Davis 1982; Gelbermann & Kemmis

1987; Bruner 1991; Best *et al.* 1993; Chaimov *et al.* 1993; Druckman *et al.* 1995; Gardosh *et al.* 2003). The interpretation of the present seismic data indicates that similar inversion took place on almost all faults underlying the fold structures of the Levantine basin and its margins (Figs 5 and 6).

Various workers suggested that the folding of the Syrian Arc is associated with closing of the Neotethys Ocean and collision of the African–Arabian and Eurasian plates. Our results further indicate an important association between the Syrian Arc deformation and the deep structure of the Levantine basin. The depth map of the top of supersequence B (Fig. 8b) and the isopach map of supersequence C (Fig. 7c) show that the uplifted and highly deformed Syrian Arc fold belt terminates sharply along a NE–SW-trending line located 50–70 km west of the present-day coastline. The western edge of the belt correlates well with a line of separation between the two main crustal units of the Levantine basin, as defined by deep-refraction, gravity and magnetic data (Fig. 8b; Ben-Avraham *et al.* 2002).

Most of the Syrian Arc contractional deformation occurs within the continental-type crust on the eastern margin, whereas the area of thinned crust to the west is considerably less deformed. It is suggested that the distribution of the Syrian Arc deformation as well as the considerable uplift of the Syrian fold belt (Figs 5 and 8b) are controlled by variations in the physical properties of the crust underlying the Levantine basin and its margin. A more comprehensive analysis of this relation is beyond the scope of the present study.

Finally, the western edge of the Syrian Arc fold belt correlates also with the Pelusium Line, as defined by Neev's *et al.* (1976). However, Neev's suggestion that this lineament is a megashear zone is not supported by our findings.

Summary and conclusions

(1) The Levantine basin is a 15 km deep basin that came into existence during Early Mesozoic, Neotethyan rifting. Faulting took place during the Anisian (Mid-Triassic) and continued through the Liassic, Bajocian and Bathonian (Early–Mid-Jurassic). Normal faulting ceased during the Mid- to Late Jurassic.

(2) The basin opened through break-up and extension in a NW–SE direction, accompanied by a strike-slip motion along its southern margin. Extension in this direction does not require the existence of compensation by a north–south-oriented transform fault along the Levant shoreline.

(3) No indications of sea-floor spreading were found in the Levantine basin. Thick accumulations of Upper Triassic to Liassic volcanic rocks in the northeastern part of the basin show no MORB characteristics.

(4) The Eratosthenes Seamount may have been the basin's western margin. The basin is an intracontinental rift, which reached only an early magmatic phase, associated with the nucleation of an oceanic spreading centre. High-velocity basement in the centre of the basin is interpreted as thinned and intruded continental crust

(5) The contractional features of the Syrian Arc fold belt were formed by the inversion of movement on pre-existing normal faults at the eastern margin of the basin. The folding occurred in several pulses starting in the Senonian and ceasing in the Miocene.

(6) The distribution of the Syrian Arc deformation was controlled by basement properties. The deformation occurs predominantly within the area underlain by continental crust.

(7) The western limit of the main fold belt, located 50–70 km west of the coastline, coincides with a zone of transition in basement properties, previously described as the Pelusium Line.

(8) The Messinian evaporitic basin was limited in the east by the uplifted fold belt composed of older strata of Oligocene to Mid-Miocene age. During highstand episodes of the Messinian sea, evaporites were deposited on the higher slope and within canyons incised into the shelf.

(9) The Plio-Pleistocene basinward progradation of the shelf break by some 20 km across the drowned Mesozoic shelf break was caused by the high sedimentation rates of both Nile and locally derived sediments. These rates exceeded the accommodation space created by the rise of the Pliocene sea level and by local subsidence.

The authors would like to thank B. Buchbinder and A. Flexer for comprehensive reviews of the manuscript and their most helpful remarks. We would like to thank the Israeli Ministry of Infrastructure for allowing us the use of the well and seismic dataset.

References

Aal, A. A., El Barkooky, A., Gerrits, M., Meyer, H. Schwander, M. & Zaki, H. 2000. Tectonic evolution of the eastern Mediterranean Basin and

its significance for hydrocarbon prospectivity in the ultra-deepwater of the Nile Delta. *The Leading Edge*, **19**(10), 1086–1102.

ALMOGI-LABIN, A., BEIN, A. & SASS, E. 1993. Late Cretaceous upwelling system along the southern Tethys margin (Israel): interrelationship between productivity, bottom water environments and organic matter preservation. *Paleoceanography*, **8**, 671–690.

AVEDIK, F., NICOLICH, R., HIRN, A., MALTEZOU, F., MCBRIDE, J., CERNOBORI, L. & the STREAMERS/PROFILES Group 1995. Appraisal of a new, high-energy and low frequency seismic pulse generating method on a deep seismic reflection profile on the Central Mediterranean Sea. *First Break*, **13**, 277–290.

BALL, M. W. & BALL, D. 1953. Oil prospects of Israel. *American Association of Petroleum Geologists Bulletin*, **37**, 1–113.

BARTOV, Y. 1974. *A structural and paleogeographical study of the central Sinai faults and domes*. PhD thesis, Hebrew University, Jerusalem (in Hebrew with English abstract).

BEIN, A. & GVIRTZMAN, G. 1977. A Mesozoic fossil edge of the Arabian plate along the Levant coastline and its bearing on the evolution of the eastern Mediterranean. *In*: BIJU-DUVAL, B. & MONTADERT, L. (eds.) *Structural History of the Mediterranean Basins*. Technip, Paris, 95–110.

BEN-AVRAHAM, Z. 1989. Multiple opening and closing of the eastern Mediterranean and south China Basin. *Tectonics*, **8**, 351–362.

BEN-AVRAHAM, Z. & GRASSO, M. 1991. Crustal structure variations and transcurrent faulting at the eastern and western margins of the eastern Mediterranean. *Tectonophysics*, **196**, 269–277.

BEN-AVRAHAM, Z. & TIBOR, G. 1994. Structure and tectonics of the Eastern Cyprean arc. *Terra abstracts suppl. 1 to Terra Nova*, **5**, 254.

BEN-AVRAHAM, Z., SHOHAM, Y. & GINZBURG, A. 1976. Magnetic anomalies in the eastern Mediterranean and the tectonic setting of the Eratosthenes Seamount. *Geophysical Journal of the Royal Astronomical Society*, **45**, 105–123.

BEN-AVRAHAM, Z., TIBOR, G., LIMONOV, A. F., LEYBOV, M. B., IVANOV, M. K., TOKAREV, M. YU. & WOODSIDE, J. M. 1995. Structure and tectonics of the eastern Cyprean Arc. *Marine and Petroleum Geology*, **12**, 263–271.

BEN-AVRAHAM, Z., GINZBURG, A., MAKRIS, J. & EPPELBAUM, L. 2002. Crustal structure of the Levant Basin, eastern Mediterranean. *Tectonophysics*, **346**, 23–43.

BEN-GAI, Y. 1996. *Sequence stratigraphy of the Plio-Pleistocene in the continental margin of the southern Levant*. PhD thesis, Tel Aviv University.

BENTOR, Y. K. & VROMAN, A. 1954. A structural contour map of Israel (1;250 000), with remarks on its dynamic interpretation. *Bulletin of the Research Council, Israel*, **4**, 125–235.

BENTOR, Y. K. & VROMAN, A. 1960. *The geological map of Israel (1:100 000). Sheet 16: Mount Sdom, explanatory text*. Geological Survey of Israel.

BEST, J. A., BARAZANGI, M., AL-SAAD, D., SAWAF, T. & GEBRAN, A. 1993. Continental margin evolution of the Northern Arabian Platform in Syria. *American Association of Petroleum Geologists Bulletin*, **77**, 173–193.

BEYDOUN, Z. R. 1988. *The Middle East: Regional Geology and Petroleum Resources*. Scientific Press, Beaconsfield, UK.

BOHANNON, R. G. & EITTREIM, S. L. 1991. Tectonic development of passive continental margins of the southern and central Red Sea with a comparison of Wilkes Land, Antarctica. *Tectonophysics*, **198**, 129–154.

BRUNER, I. 1991. *Investigation of the subsurface in the northern Negev, Israel, using seismic reflection techniques*. PhD thesis, Tel Aviv University.

BUCHBINDER, B. & SIMAN-TOV, R. 2000. Oligocene clastics in the Ashdod area: mass flow and turbidite deposits in a submarine-fan setting. *Israel Geological Society Annual Meeting* (abstract), Ma'alot, 25.

BUCHBINDER, B. & ZILBERMAN, E. 1997. Sequence stratigraphy of Miocene–Pliocene carbonate–siliciclastic shelf deposits in the eastern Mediterranean margin (Israel): effects of eustasy and tectonics. *Sedimentary Geology*, **112**, 7–32.

BUCHBINDER, B., BENJAMINI, C., MIMRAN, Y. & GVIRTZMAN, G. 1988. Mass transport in Eocene pelagic chalk on the northwestern edge of the Arabian platform, Shefela area, Israel. *Sedimentology*, **35**, 257–274.

BUCHBINDER, B., BENJAMINI, C. & LIPSON-BNITAH, S. 2000. Sequence development of Late Cenomanian–Turonian carbonate ramps, platforms and basins of Israel. *Cretaceous Research*, **21**, 813–843.

CHAIMOV, T. A., BARAZANGI, M., AL-SAAD, D., SAWAF, T. & KHADDOURI, M. 1993. Seismic fabric and 3-D structure of the southwestern intracontinental Palmyride fold belt, Syria. *American Association of Petroleum Geologists Bulletin*, **77**, 2032–2047.

COCHRAN, J. R. 2001. Nucleation of an oceanic spreading center in a continental rift: the northern Red Sea. http://www.copernicus.org/EGS/egsga/Nice01/programme/abstracts/aai1791.pdf.

COHEN, Z. 1976. Early Cretaceous buried canyon: influence on accumulation of hydrocarbons in the Helez oil field, Israel. *American Association of Petroleum Geologists Bulletin*, **60**, 108–114.

COHEN, Z., FLEXER, A. & KAPTSAN, V. 1988. The Pleshet basin, a newly discovered link in the peripheral chain of basins of the Arabian craton. *Journal of Petroleum Geology*, **11**(4), 403–414.

COHEN, Z., FLEXER, A. & KAPTSAN, V. 1990. The tectonic mosaic of the southern Levant: Implication for hydrocarbon prospects. *Journal of Petroleum Geology* **13**(4), 437–462.

DAVIS, B. K. 1982. *Structural inversion in Europe and Israel and its importance in oil exploration*. Oil Exploration (Invest.) Ltd Report **OEL/82/04**.

DERCOURT, J., ZONENSHAIN, L. P., RICOU, L. E, *et al.* 1986. Geological evolution of the Tethys belt from the Atlantic to the Pamirs since the Lias. *Tectonophysics*, **123**, 241–315.

DERIN, B. 1974. *The Jurassic of central and northern Israel*. PhD thesis, Hebrew University, Jerusalem.

DERIN, B., GERRY, E. & LIPSON, S. 1982. Asher Atlit-1, northern coastal plain, stratigraphic log. Israel Institute of Petroleum and Energy Report 2/82.

DERIN, B., LIPSON, S. & GERRY, E. 1990. *Microbiostratigraphy and environments of deposition of the Yam 2 offshore well*. Israel Institute of Petroleum and Energy Report **5/90**.

DE SITTER, L. U. 1962. Structural development of the Arabian Shield in Palestine. *Geologie en Mjnibouw*, **11**, 116–124.

DEWEY, J. F., PITMAN, W. C., III, RYAN, W. B. F. & BONIN, J. 1973. Plate tectonics and the evolution of the Alpine system. *Geological Society of America Bulletin*, **84**, 3137–3180.

DRUCKMAN, Y. 1977. Differential subsidence during the deposition of the Lower Jurassic Ardon Formation in western Jordan, southern Israel and northern Sinai. *Israel Journal of Earth Sciences*, **26**, 45–54.

DRUCKMAN, Y. 1981. Comments on the structural reversal model as a factor of the geological evolution of Israel. *Israel Journal of Earth Sciences*, **30**, 44–48.

DRUCKMAN, Y. 1984. Evidence for Early–Middle Triassic faulting and possible rifting from the Helez Deep borehole and the coastal plain of Israel, *In*: DIXON, J. E. & ROBERTSON, A. H. F. (eds) *The Geological Evolution of the Eastern Mediterranean*. Geological Society, London, Special Publications, **17**, 203–212.

DRUCKMAN, Y., CONWAY, B., ESHET, Y., *et al.* 1994. *The stratigraphy of the Yam Yafo-1 borehole*. Geological Survey of Israel Report **GSI/28/94**.

DRUCKMAN, Y., GILL, D., FLEISCHER, L., GELBERMANN, E. & WOLFF, O. 1995. Subsurface geology and structural evolution of the northwestern Negev, southern Israel. *Israel Journal of Earth Science*, **44**, 115–136.

DVORKIN, A. & KOHN, B. P. 1989. The Asher Volcanics, northern Israel: petrography, mineralogy and alteration. *Israel Journal of Earth Sciences*, **38**, 105–123.

EL-ISA, Z. H., MECHIE, J., PRODEHL, C., MAKRIS, J. & RIHM, R. 1987. A crustal structure study in Jordan derived from seismic refraction data. *Tectonophysics*, **138**, 235–253.

EMERY, D. & MYERS, K. 1996. *Sequence Stratigraphy*. Blackwell Science, Oxford.

EYAL, Y. & RECHES, Z. 1983. Tectonic analysis of the Dead Sea rift region since the Late Cretaceous based on mesostructures. *Tectonics*, **2**, 167–185.

FINETTI, I. 1985. Structure and evolution of the central Mediterranean (Pelagian and Ionian Seas). *In*: STANLEY, D. J. & WEZEL, F. C. (eds) *Geological Evolution of the Mediterranean Basin*. Springer, Berlin, 215–230.

FLEXER, A. 1968. Stratigraphy and facies development of Mount Scopus Group (Senonian–Paleocene) in Israel and adjacent countries. *Israel Journal of Earth Sciences*, **17**, 85–114.

FLEXER, A., ROSENFELD, A., LIPSON-BENITAH, S. & HONIGSTEIN, A. 1986. Relative sea level changes during the Cretaceous in Israel. *American Association of Petroleum Geologists Bulletin*, **70**, 1685–1699.

FOLKMAN, Y. & BEN-GAI, Y. 2004. The Jonah buried Seamount: intrusive structure in the southeastern Levant Basin, offshore Israel. *Israel Geological Society Annual Meeting* (abstract).

FREUND, R., GOLDBERG, M., WEISSBROD, T., DRUCKMAN, Y. & DERIN, B. 1975. *The Triassic–Jurassic structure of Israel and its relation to the origin of the eastern Mediterranean*. Geological Survey of Israel Bulletin, **65**.

GARDOSH, M. 2002. *The sequence stratigraphy and petroleum systems of the Mesozoic, southeastern Mediterranean continental margin*. PhD thesis, Tel Aviv University.

GARDOSH, M., BRUNER, I., DRUCKMAN, Y., REZNIKOV, M., BUCHBINDER, B. & SAGY, Y. 2003. Mesozoic tectonic phases and hydrocarbon potential of the southeastern Mediterranean basin. Results from new, offshore seismic surveys. *Israel Geological Society Annual Meeting* (abstract), Ein Boqeq, 39.

GARFUNKEL, Z. 1978. The Negev—regional synthesis of sedimentary basins. *In*: *10th International Congress of Sedimentology, Guidebook, Part I*, 34–110.

GARFUNKEL, Z. 1989. Tectonic setting of Phanerozoic magmatism in Israel. *Israel Journal of Earth Science*, **38**, 51–74.

GARFUNKEL, Z. 1998. Constraints on the origin and history of the eastern Mediterranean basin. *Tectonophysics*, **298**, 5–35.

GARFUNKEL, Z. 2004. Origin of the Eastern Mediterranean basin: a reevaluation. *Tectonophysics*, **391**, 11–34.

GARFUNKEL, Z. & DERIN, B. 1984. Permian–Early Mesozoic tectonism and continental margin formation in Israel and its implications to the history of the eastern Mediterranean. *In*: DIXON, J. E. & ROBERTSON, A. H. F. (eds) *The Geological Evolution of the Eastern Mediterranean*. Geological Society, London, Special Publications, **17**, 18–201.

GELBERMANN, E. 1995. *Revised seismic structural and isopach maps, central and southern Israel*. Institute for Petroleum Research and Geophysics Report **201/22/88–94**.

GELBERMANN, E. & KEMMIS, J. L. 1987. Triassic to Late Cretaceous tectonic alignments in the southern coastal plain and the northwestern Negev. *Israel Geological Society Annual Meeting* (abstract), Mizpe Ramon, 39.

GILL, D., CONWAY, B. H., ESHET, Y., LIPSON, S., PERELIS-GROSSOWICZ, L., ROSENFELD, A. & SIMANTOV, R. 1995. *The stratigraphy of the Yam West 1 borehole*. Geological Survey of Israel Report **GSI/13/95**.

GINZBURG, A. & BEN-AVRAHAM, Z. 1987. The deep structure of the central and southern Levant continental margin. *Annales Tectonicae*, **1**, 105–115.

GINZBURG, A. & FOLKMAN, Y. 1980. The crustal structure between the Dead Sea rift and the Mediterranean Sea. *Earth and Planetary Science Letters*, **51**, 181–188.

GINZBURG, A., COHEN, S. S., HAY-RAY, H. & ROZENZWEIG, A. 1975. Geology of the Mediterranean shelf of Israel. *American Association of Petroleum Geologists Bulletin*, **59**, 2142–2160.

GINZBURG, A., MAKRIS, J., FUCHS, K., PRODEHL, C., KAMINSKI, W. & AMITAI, U. 1979. A seismic study of the crust and upper mantle of the Jordan–Dead Sea rift and their transition towards the Mediterranean Sea. *Journal of Geophysical Research*, **84**, 1569–1582.

GRADMANN, S., HUBSCHER, C., BEN-AVRAHAM, Z., GAJEWSKI, B. & NETZEBAND, G. 2005. Salt tectonics off northern Israel. *Marine and Petroleum Geology*, **22**, 597–611.

GVIRTZMAN, G. 1970. *The Saqiye Group (Late Eocene to Early Pleistocene) in the Coastal Plain and Hashephela regions, Israel*. Geological Survey of Israel Report **OD/5/67**.

GVIRTZMAN, G. & BUCHBINDER, B. 1978. The Tertiary history of the coastal plain and continental shelf of Israel and its bearing on the history of the Eastern Mediterranean. *In*: ROSS, D. A., NEPROCHNOV, Y. P., *et al.* (eds) *Initial Reports of the Deep Sea Drilling Project, 42B*. US Government Printing Office, Washington, DC, 1195–1222.

GVIRTZMAN, G. & REISS, Z. 1965. *Stratigraphic nomenclature in the Coastal Plain and Hashephela regions*. Geological Survey of Israel Report **OD/1/65**.

GVIRTZMAN, G. & STEINITZ, G. 1983. The Asher Volcanics—an Early Jurassic event in northern Israel. *Israel Geological Survey Current Research*, 28–33.

HAQ, B. U., HARDENBOL, J. & VAIL, P. R. 1988. Mesozoic and Cenozoic chronostratigraphy and cycles of sea-level changes. *In*: WILGUS, C. K., HASTINGS, B. S., KENDALL, C. G., POSAMENTIER, H. W., ROSS, C. A. & WAGONER, J. C. (eds) *Sea-level Changes: an Integrated Approach*. Society of Sedimentary Geology, Special Publications, **42**, 71–108.

HIRSCH, F., FLEXER, A., ROSENFELD, A. & YELLIN-DROR, A. 1995. Palinspastic and crustal setting of the eastern Mediterranean. *Journal of Petroleum Geology*, **18**(2), 149–170.

HIRSCH, F., BASSOULLET, J. P., CARIOU, E., *et al.* 1998. The Jurassic of the southern Levant: biostratigraphy, palaeogeography and cyclic event. *In*: CRASQUIN-SOLEAU, S. & BARRIER, E. (eds) *Peri-Tethys Memoir 4: Epicratonic Basins of Peri-Tethyan Platforms*. Mémoires du Museum National d'Histoire Naturelle, **179**, 213–235.

HOROWITZ, A. 1979. *The Quaternary of Israel*. Academic Press, New York.

HSÜ, K. J., RYAN, W. B. F. & CITA, M. B. 1973. Late Miocene desiccation of the Mediterranean. *Nature*, **242**, 240–244.

HSÜ, K. J., MONTADERT, L., BERNOULLI, D., *et al.* 1978. History of the Mediterranean salinity crisis. *In:* HSÜ, K., MONTADERT, L., *et al. Initial Reports of the Deep Sea Drilling Project, 42A*. US Government Printing Office, Washington, DC, 1053–1078.

KLITGORD, K. D. & HUTCHINSON, D. R. 1988. U.S. Atlantic continental margin; structural and tectonic framework. *In*: SHERIDAN, R. E. & GROW, J. A. (eds) *The Atlantic Continental Margin, U.S.* Geological Society of America, The Geology of North America, **I–2**, 19–55.

KOHN, B. P., LANG, B. & STEINITZ, G. 1993. $^{40}Ar/^{39}Ar$ dating of the Atlit one volcanic sequence, northern Israel. *Israel Journal of Earth Science*, **42**, 17–23.

KORNGREEN, D. 2004. *The Triassic in northern Israel*. PhD thesis, Ben Gurion University, Beer-Shevu.

KRENKEL, E. 1924. Der Syrische Bogen. *Zentralblatt Mineralogie*, **9**, 274–281; and **10**, 301–313.

LOVELOCK, P. E. R. 1984. A review of the tectonics of the northern Middle East region. *Geological Magazine*, **121**, 577–587.

MAKRIS, J. & WANG, J. 1994. Bouguer gravity anomalies of the Eastern Mediterranean Sea. *In*: KRASHENINIKOV, V. A. & HALL, J. K. (eds) *Geological structure of the north-eastern Mediterranean (Cruise 5 of the Research Vessel* Akademik Nikolaj Strakhov*)*. Historical Productions–Hall, Jerusalem, 87–98.

MAKRIS, J., BEN-AVRAHAM, Z., BEHLE, A., *et al.* 1983. Seismic refraction profiles between Cyprus and Israel and their interpretation. *Geophysical Journal of the Royal Astronomical Society*, **75**, 575–591.

MART, Y. & ROBERTSON, A. H. F. 1998. Eratosthenes Seamount: an oceanic yardstick recording the Late Mesozoic–Tertiary geological history of the eastern Mediterranean. *In*: ROBERTSON, A. H. F., EMEIS, K. C. RICHTER, C. & CAMERLENGHI, A. (eds) *Proceedings of the Ocean Drilling Program, Scientific Results*, 160. Ocean Drilling Program, College Station, TX, 701–708

MARTINEZ, F. & COCHRAN, J. R. 1988. Structure and tectonics of the Red Sea: catching a continental margin between rifting and drifting. *Tectonophysics*, **150**, 1–32.

MCBRIDE, J. H., BARAZANGI, M., BEST, J., AL-SAAD, D., SAWAF, T., AL-OTRI, M. & GEBRAN, A. 1990. Seismic reflection structure of intracratonic Palmyrid fold–thrust belt and surrounding Arabian Platform, Syria. *American Association of Petroleum Geologists Bulletin*, **74**, 238–259.

NEEV, D. 1977. The Pelusium Line—a major transcontinental shear. *Tectonophysics*, **38**, T1–T8.

NEEV, D., ALMAGOR, G., ARAD, A., GINZBURG, A. & HALL, J. K. 1976. *The geology of the southeastern Mediterranean*. Geological Survey of Israel Bulletin, **68**.

PICARD, L. 1943. Structure and evolution of Palestine with comparative notes on neighboring countries. *Bulletin, Geological Department, Hebrew University*, **4**, 1–143.

PICARD, L. 1959. *Geology and oil exploration of Israel*. Bulletin of the Research Council in Israel, **G8**, 1–30.

ROBERTSON, A. H. F. 1998. Mesozoic–Tertiary tectonic evolution of the easternmost Mediterranean area: integration of marine and land evidence. *In*: ROBERTSON, A. H. F., EMEIS, K. C., RICHTER, C. & CAMERLENGHI, A. (eds) *Proceedings of the Ocean Drilling Program, Scientific Results, 160*, Ocean Drilling Program, College Station, TX, 723–782.

ROBERTSON, A. H. F. & DIXON, J. E. 1984. Introduction: aspects of the geological evolution of the eastern Mediterranean. *In*: DIXON, J. E. & ROBERTSON, A. H. F. (eds.) *The Geological Evolution of the Eastern Mediterranean*. Geological Society, London, Special Publications, **17**, 1–74.

ROUCHY, J. M. & SAINT MARTIN, J. P. 1992. Late Miocene events in the Mediterranean as recorded by carbonate–evaporite relations. *Geology*, **20**, 629–632.

RYAN, W. B. F. 1978. Messinian badlands on the southeastern margin of the Mediterranean Sea. *Marine Geology*, **27**, 349–363.

RYBAKOV, M. & SEGEV, A. 2004. Top of the crystalline basement in the Levant. *Geochemistry, Geophysics and Geodynamics*, **5**, 1–8.

RYBAKOV, M., GOLDSHMIT, V. & ROTSTEIN, Y. 1997. New regional gravity and magnetic maps of the Levant. *Geophysical Research Letters*, **24**, 33–36.

SASS, E. & BEIN, A. 1982. The Cretaceous carbonate platform in Israel. *Cretaceous Research*, **3**, 135–144.

ŞENGÖR, A. M., YILMAZ, Y. & SUNGURLU, O. 1984. Tectonics of the Mediterranean Cimmerides: nature and evolution of the western termination of Paleo-Tethys. *In*: DIXON, J. E. & ROBERTSON, A. H. F. (eds) *The Geological Evolution of the Eastern Mediterranean.* Geological Society, London, Special Publications, **17**, 77–112.

STAMPFLI, G. M., MOSAR, J., FAVRE, P. A., PILLEVUIT, A. & VANNAY, J.-C. 2001. Permo-Mesozoic evolution of the western Tethyan realm: the Neotethys East-Mediterranean Basin connection. *In*: ZIEGLER, P. A., CAVAZZA, W., ROBERTSON, A. H. F. & CRASQUIN-SOLEAU, S. (eds) *Peri-Tethys Memoir 6: Peri-Tethyan Rift/Wrench Basins and Passive Margins*. Mémoires du Museum National d'Histoire Naturelle, **186**, 51–108.

STEINITZ, G., GVIRTZMAN, G. & LANG, B. 1983. Evaluation of K–Ar ages of the Asher volcanics. *Geological Survey of Israel, Current Research 1982*, 34–38.

WOODSIDE, J. M. 1977. Tectonic elements and crust of the eastern Mediterranean Sea. *Marine Geophysical Researches*, **3**, 317–354.